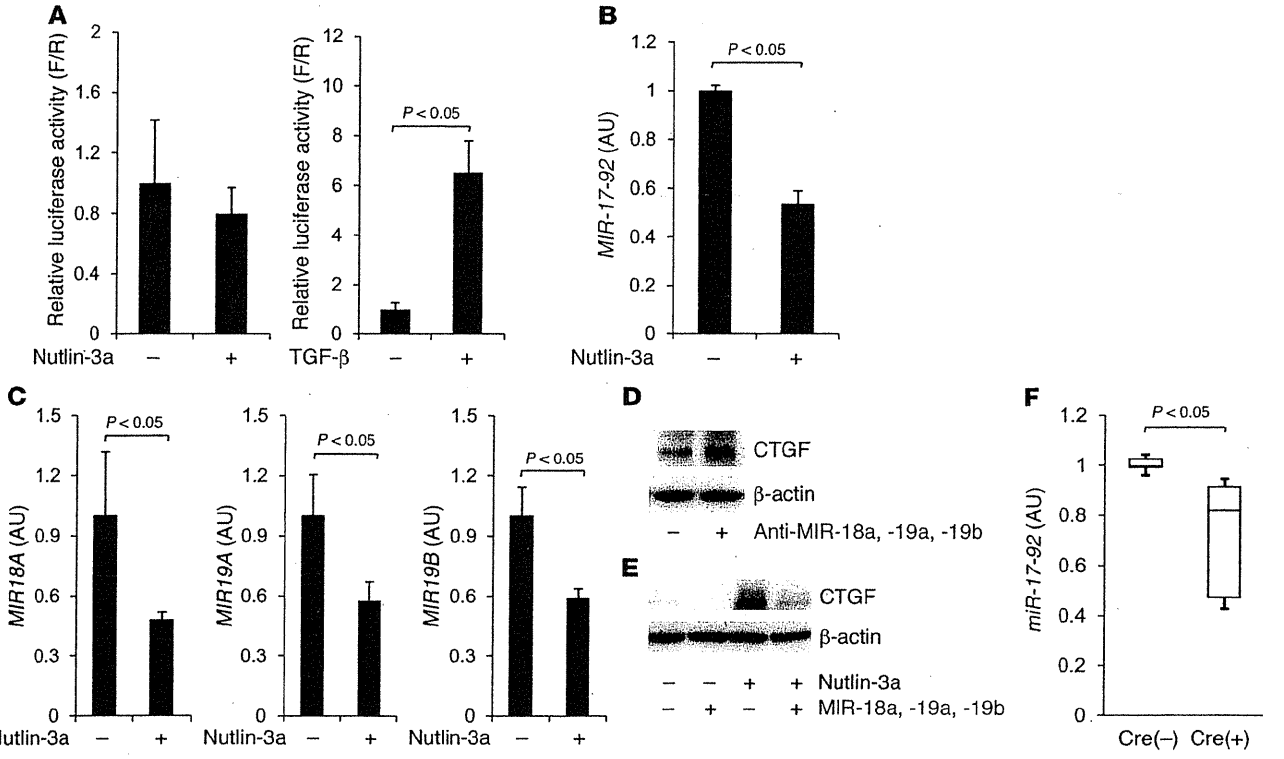

Figure 8

p53 activation upregulates CTGF synthesis via repression of the *miR-17-92* cluster gene. (**A**) HepG2 cells (1.0×10^5) were cotransfected with pTS-589 and pRL-TK for 48 hours and treated with nutlin-3a (20 μM) or recombinant TGF-β (10 ng/ml) for 24 hours. Firefly luciferase and *Renilla* luciferase activity was measured and is presented as relative luminescence values for firefly luciferase versus *Renilla* luciferase (F/R). $n = 4$/group. (**B** and **C**) HepG2 cells (1.0×10^5) were treated with nutlin-3a (20 μM) or vehicle for 24 hours. (**C**) Real-time RT-PCR analysis of *miR-17-92* mRNA (**B**), *MIR18A*, *MIR19A*, and *MIR19B* miRNA expression; $n = 3$/group. Statistical analyses were performed by the paired *t* test (**A**–**C**). (**D**) HepG2 cells were transfected with a mixture of antisense of *MIR18A*, *MIR19A*, and *MIR19B* at 100 nM each or negative control at 300 nM for 2 days. Expression of CTGF protein was assessed by Western blotting. (**E**) HepG2 cells were transfected with a mixture of precursor of *MIR18A*, *MIR19A*, and *MIR19B* at 10 nM each or negative control at 30 nM for 2 days and cultured with nutlin-3a (20 μM) or vehicle for 24 hours. Expression of CTGF protein was assessed by Western blotting. (**F**) Expression of *miR-17-92* mRNA in isolated hepatocytes was assessed by real-time RT-PCR. Cre(+), $Mdm2^{fl/fl}$*alb-cre*; cre(–), $Mdm2^{fl/fl}$; 5 mice per group.

products, represented by p21 (Figure 7C), indicating that nutlin-3a could activate p53 in these cells. Upon nutlin-3a treatment, *CTGF* gene expression increased in a time-dependent manner in HepG2 cells (Figure 7D), while *TGFB1* and *PDGFB* gene expression did not (Supplemental Figure 7). We also observed that CTGF protein levels gradually increased upon nutlin-3a treatment (Figure 7C). Adriamycin, a DNA-alkylating agent, could also activate p53, leading to upregulation of CTGF mRNA and protein levels in HepG2 cells in a time-dependent manner (Figure 7, E and F). Administration of *p53* siRNA into HepG2 cells efficiently reduced p53 expression, which was demonstrated by the mRNA levels (Supplemental Figure 8) and protein levels (Figure 7G), and inhibited upregulation of p21 protein upon treatment with nutlin-3a and Adriamycin (Figure 7G). Under this condition, p53 knockdown completely abolished the increase in CTGF that had resulted from administration of these drugs (Figure 7, G and H). These results clearly demonstrated that the increase in CTGF synthesis by nutlin-3a or Adriamycin was completely dependent on p53 in HepG2 cells, indicating that p53 positively regulates CTGF synthesis in human hepatocytes. To directly demonstrate the effect of p53 on CTGF expression in vivo, we injected a p53 expression plasmid, ORF9-mp53, or its control plasmid into BALB/c mice via the tail vein by a hydrodynamic injection procedure (28) and examined *Ctgf* gene expression 2 days later. Although hydrodynamic injection of the p53 expression plasmid only led to nuclear expression of p53 in hepatocytes at a rate of approximately 5% (Supplemental Figure 9A), it significantly increased *Ctgf* gene expression in the liver compared with the control hydrodynamic injection (Supplemental Figure 9B). These results also demonstrated the existence of the p53/CTGF pathway in vivo.

p53 activation upregulates CTGF synthesis via repression of the miR-17-92 cluster gene. Next, we tried to elucidate the molecular mechanism underlying CTGF regulation by p53 in HepG2 cells. To examine whether p53 transcriptionally upregulates *CTGF* gene expression, we introduced plasmid pTS-589 — which contains the *CTGF* promoter from 802 base pairs upstream of the transcript start site to 22 base pairs downstream of the coding sequence linked to the upstream of a firefly luciferase reporter gene (29) — into HepG2 cells. Then, we evaluated the transcription activity of the *CTGF* promoter upon treatment with nutlin-3a or recombinant TGF-β, which is known to transcriptionally upregulate CTGF (29). Whereas luciferase activity increased upon TGF-β treatment, it did not

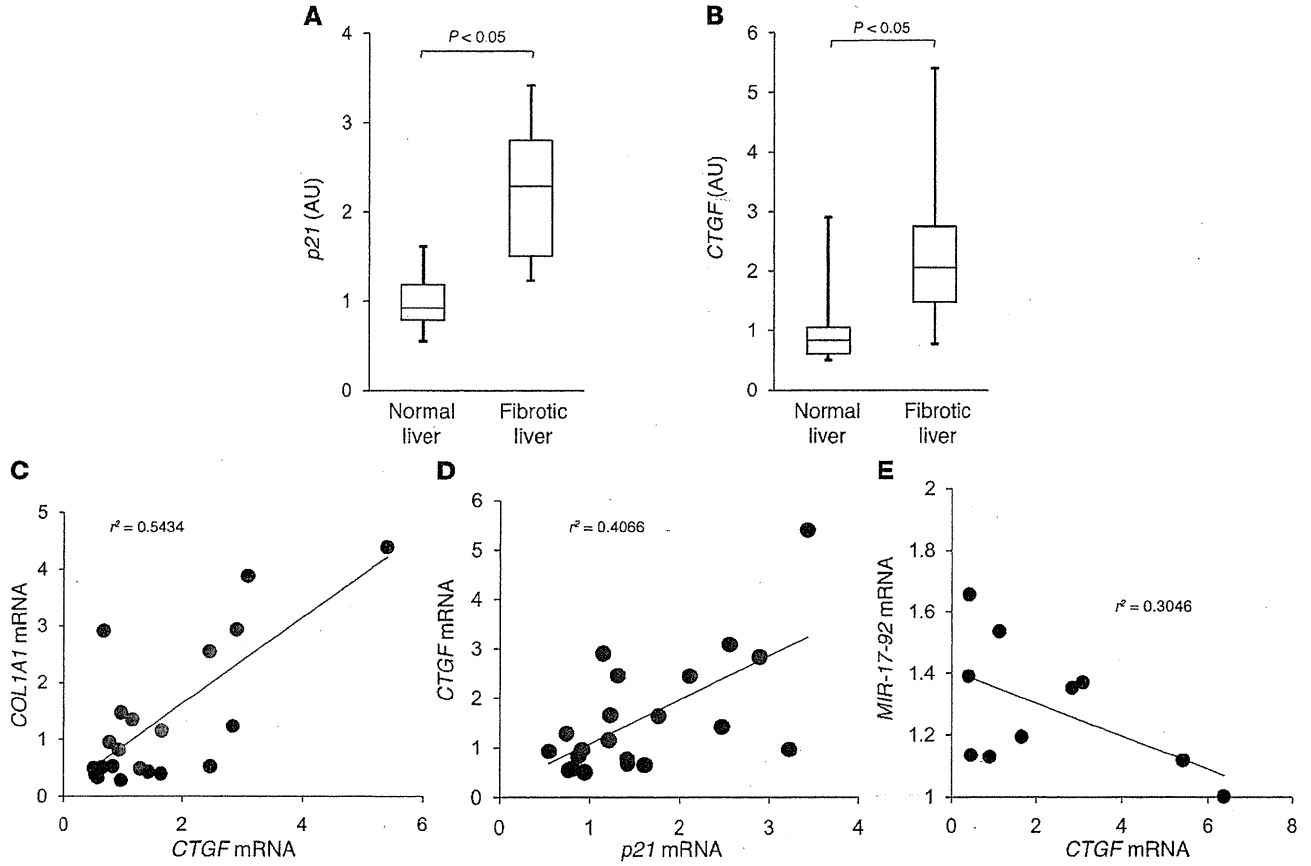

Figure 9

p53-regulated gene expression increases in fibrotic human liver and is correlated with an increase in *CTGF* gene expression. (**A** and **B**) A total of 21 non-tumorous human liver samples were subdivided into two groups histologically defined as normal liver and fibrotic liver. *p21* (**A**) and *CTGF* (**B**) mRNA levels in the liver were determined by real-time RT-PCR; $n = 11$ (normal liver group) and $n = 10$ (fibrotic liver group). (**C** and **D**) *COL1A1*, *CTGF*, and *p21* mRNA levels in the liver of 21 non-tumorous human liver samples were determined by real-time RT-PCR and plotted to analyze the correlation between *COL1A1* and *CTGF* ($P < 0.01$) (**C**) or between *CTGF* and *p21* ($P < 0.01$) (**D**). (**E**) *miR-17-92* and *CTGF* mRNA levels in the liver of 10 human fibrotic liver samples were determined by real-time RT-PCR and plotted to analyze the correlation between them ($P < 0.01$).

change upon nutlin-3a treatment in HepG2 cells (Figure 8A), suggesting that the post-transcriptional regulation may be involved in the p53-induced CTGF upregulation. Recently, epigenetic regulation of the *CTGF* gene has been demonstrated (30–32), and the *miR-17-92* cluster gene, in particular, has been reported to repress CTGF synthesis in murine colonocytes and human glioblastoma cells (31, 32). Upon nutlin-3a treatment, expression of the *miR-17-92* cluster gene decreased in HepG2 cells (Figure 8B), indicating that p53 activation reduced *MIR-17-92* gene expression in HepG2 cells. The miR-17-92 cluster comprises 7 miRNAs that are transcribed as a single polycistronic unit (31, 33), and in silico analysis revealed that, among these miRNAs, *MIR18A*, *MIR19A*, and *MIR19B* can be predicted to target CTGF. Real-time RT-PCR study revealed that the gene expression of these 3 miRNAs also decreased upon nutlin-3a treatment in HepG2 cells (Figure 8C). Introduction of the antisense of these 3 miRNAs increased CTGF synthesis in HepG2 cells (Figure 8D), indicating that they suppressed CTGF synthesis in HepG2 cells. To investigate the causal involvement of downregulation of the miRNAs in p53-induced CTGF upregulation, we administered precursors of the miRNAs to HepG2 cells, and CTGF synthesis was examined upon nutlin-3a treatment. In contrast to negative control miRNA, administration of these miRNAs inhibited the upregulation of CTGF upon nutlin-3a treatment (Figure 8E), suggesting that a decrease in miR-18a, miR-19a, and miR-19b in the *miR-17-92* cluster was involved in the mechanism of CTGF upregulation by p53. To investigate the involvement of the miR-17-92 cluster in CTGF upregulation in hepatocytes of Mdm2-knockout mice, we examined hepatocyte gene expression of the *miR-17-92* cluster and found it to be significantly lower in the knockout mice than in the control littermates (Figure 8F), suggesting that the miR-17-92 cluster may be involved in p53-mediated CTGF upregulation in hepatocytes of the knockout mice.

p53-regulated gene expression increases in the human fibrotic liver and is correlated with an increase in Ctgf gene expression. Finally, to investigate the relationship between p53 activation and human liver fibrosis, we examined the expression of p53-regulated genes and fibrosis-related genes in human liver samples. *p21* gene expression increased in the fibrotic liver and was significantly higher than in the normal liver (Figure 9A). We observed that *NOXA* gene expression in the fibrotic liver was also significantly higher than in the normal liver (Supplemental Figure 10). These findings suggested that p53 may be transcriptionally active in the fibrotic

liver. Regarding fibrosis-related genes, *CTGF* gene expression was significantly higher in the fibrotic liver than in the normal liver (Figure 9B). The increase in *CTGF* gene expression paralleled the increase in *COL1A1* gene expression, with a significant correlation between them (Figure 9C). These results suggested that CTGF may be involved in the progression of human liver fibrosis. There was a significant correlation between the gene expression of *p21* and *CTGF* (Figure 9D), suggesting that p53 activation might be involved in the upregulation of CTGF and the progression of liver fibrosis in humans. We also found that there was a significant negative correlation between the gene expression of *CTGF* and the *miR-17-92* cluster in the fibrotic liver (Figure 9E), suggesting the involvement of the miR-17-92 cluster in the p53/CTGF pathway in the human fibrotic liver.

Discussion

In the present study, to investigate the role of p53 in liver fibrosis, we generated hepatocyte-specific Mdm2-knockout mice and found a direct link between p53 activation in parenchymal cells and organ fibrosis. In unstressed cells, expression of p53 is tightly regulated and maintained at a low level by binding with a variety of proteins that promote p53 degradation via the ubiquitin/proteasome pathway (13). Among these p53 inhibitory proteins, Mdm2 is critically important for this process, since Mdm2-knockout mice show embryonic lethality but were fully rescued by deletion of *p53* (34). When Cre-mediated conditional Mdm2-knockout mice were generated and studied, the findings revealed that *Mdm2* deletion only in the central nervous system or the heart still led to embryonic lethality due to massive apoptosis, and this could also be rescued by deletion of *p53* (15, 35). These findings demonstrated that Mdm2 functions as a crucial and specific p53 inhibitor in a variety of organs. In the present study, using hepatocyte-specific Mdm2-knockout mice, we could observe the consequences of persistent p53 activation in hepatocytes and discover the profibrotic function of p53.

Regarding the mechanism(s) involving spontaneous liver fibrosis in our Mdm2-knockout mice, we observed a mild increase in hepatocyte apoptosis (Figure 3, A–E). We have previously reported that hepatocyte-specific knockout of either Bcl-xL or Mcl-1, major anti-apoptotic Bcl-2 family proteins, causes massive hepatocyte apoptosis and leads to liver fibrosis in mice (16, 36). Thus, although apoptosis is generally considered to be quiescent cell death that does not cause organ injury, hepatocyte apoptosis is apparently involved in liver fibrogenesis. However, in these mice, liver fibrosis is not evident at 6 weeks of age, although they show much higher ALT levels, more than 300 IU/ml, and seem to have much more apoptosis than hepatocyte-specific Mdm2-knockout mice. Moreover, when hepatocyte apoptosis was similarly induced in Mdm2-knockout mice and control littermates by administration of ABT-737, a Bcl-xL inhibitor that causes mild hepatocyte apoptosis in vivo (refs. 21, 22, and Supplemental Figure 11A), additional liver fibrogenic responses occurred in the knockout mice but not in the control littermates (Supplemental Figure 11B). Based on these findings, hepatocyte apoptosis could contribute to liver fibrosis, but some additional factors should be required for the liver fibrosis observed in the Mdm2-knockout mice.

In Mdm2-knockout mice, we also found an upregulation of CTGF synthesis in hepatocytes (Figure 7, A and B). CTGF, also known as CCN family 2 (CCN2), is one of the CCN family proteins and plays a pivotal role in fibrosis in the lung, skin, kidney, and heart (37) through extracellular matrix production, cell cycle control, and cell adhesion and migration (14, 38, 39). With respect to the liver, several publications have reported that CTGF expression increases in human chronic liver fibrotic diseases such as chronic hepatitis C, NASH, and liver cirrhosis (40–43). Moreover, previous studies have shown that CTGF inhibition by siRNA had a beneficial effect on experimental liver fibrosis (44, 45), indicating that CTGF functions as an important profibrogenic cytokine in the liver. Although the main source of CTGF was thought to be HSCs and fibroblasts (46), recent reports have revealed that CTGF is also produced from hepatocytes (47, 48). Furthermore, transgenic mice expressing CTGF under the control of the albumin gene promoter showed exacerbation of liver fibrosis induced by chronic CCl_4 administration (49), demonstrating that hepatocyte-derived CTGF plays an important role in liver fibrogenesis. However, Tong et al. (49) have also reported that hepatocyte-specific CTGF transgenic mice did not show spontaneous fibrosis in the liver without any fibrotic stimuli. Taken together, these findings support the idea that CTGF produced from hepatocytes may be an important factor for promoting liver fibrosis in the presence of apoptotic stimuli in Mdm2-knockout mice.

To further examine this idea, we performed an in vitro study using murine HSCs cocultured with apoptotic bodies prepared from hepatocytes. In agreement with a previous report (50), hepatocyte-derived apoptotic bodies efficiently activated HSCs (Supplemental Figure 12), and CTGF administration significantly upregulated type I collagen synthesis in HSCs in combination with apoptotic bodies (Supplemental Figure 13). Based on these results and in vivo findings, we suggest that hepatocyte p53 activation increased hepatocyte apoptosis and CTGF synthesis, and both together may induce HSC activation and collagen synthesis, contributing to the development of spontaneous liver fibrosis in Mdm2-knockout mice. It should be noted here that p53 activation did not appear to be a single causal factor for inducing apoptosis in two independent models of murine liver fibrosis but was a required for CTGF expression. Since CTGF expression was well correlated with p53 activation and liver fibrosis in human livers, p53-mediated CTGF induction may be a novel and important pathway for promoting liver fibrosis.

The Alb-Cre transgenic mice expressed cre recombinase in intrahepatic cholangiocytes as well as hepatocytes, as observed from β-galactosidase staining of the liver sections in Alb-Cre and Rosa26-LacZ double-transgenic mice (data not shown). In the present study, Mdm2-knockout mice (*Mdm2$^{fl/fl}$alb-cre*) actually showed p53 accumulation and CTGF expression in some cholangiocytes (Supplemental Figure 14 and Figure 7B), and nutlin-3a treatment upregulated *CTGF* gene expression as well as p53-regulated genes in SNU-1079 cells, a human cholangiocellular carcinoma cell line with wild-type p53 status (ref. 51 and Supplemental Figure 15), suggesting the existence of the p53/CTGF pathway in cholangiocytes as well. However, CTGF expression was observed even in the cholangiocytes of control littermates, and its levels were not much different from those of the knockout mice (Figure 7B). Therefore, although cholangiocytes may contribute to hepatic CTGF synthesis in physiological settings, they may contribute less to the hepatic CTGF increase observed in Mdm2-knockout mice.

Recent research has shown that the *CTGF* gene is repressed by several miRNAs such as miR-18a, miR-30, and miR-133 (31, 32, 52, 53). In addition, a previous report has revealed that p53 represses *miR-17-92* transcription by binding to the p53-binding

site overlapping the TATA box in the *miR-17-92* promoter lesion (54). Thus, we focused on the miR-17-92 cluster (which includes miR-18) and identified a what we believe to be a novel regulatory mechanism by which p53 upregulates CTGF through repression of the *miR-17-92* cluster gene in hepatocytes, revealing the involvement of this mechanism not only in vitro, but also in rodents and fibrotic human liver.

In the present study, we demonstrated a direct causal link between p53 activation in hepatocytes and liver fibrosis, as evidenced by the spontaneous liver fibrosis of hepatocyte-specific Mdm2-knockout mice and the alleviation of diet- or TAA-induced liver fibrosis in hepatocyte-specific p53-knockout mice. In hepatocytes, p53 activation induced the expression of CTGF, a key regulator of liver fibrosis, through miRNA regulation. Analysis of human tissues provided evidence that the p53/CTGF axis may be involved in human liver fibrosis. Recently, therapeutic applications of a p53 inhibitor have been proposed for preventing radiation-induced adverse events that are mediated by p53 activation (55). CTGF was also reported to increase in a variety of tissues, such as the liver, intestine, and colon, upon irradiation (56, 57) and play an important role in the progression of radiation-induced fibrosis (57, 58). Our present study suggests the possibility that positive regulation of CTGF by p53 may be a therapeutic target of organ fibrosis caused by irradiation therapy as well as disease.

Methods

Cell lines and materials. Human hepatoma cell line HepG2 and murine normal hepatocyte cell line BNL CL.2 were obtained from ATCC, and human cholangiocellular carcinoma cell line SNU-1079 was obtained from the Korean Cell Line Bank (51). They were cultured at 37°C under 5% CO_2 in DMEM containing 10% FCS (Sigma-Aldrich). Nutlin-3a and Adriamycin were purchased from Sigma-Aldrich.

Human samples. Non-tumorous liver samples were obtained from 21 patients at surgical operation for hepatocellular carcinoma (HCC) (n = 10) and colorectal liver metastasis (n = 11). Among the 10 patients with HCC, 7 were positive for HCV antibody. Of the 10 patients, 4 were histologically diagnosed as having liver cirrhosis and 6 as having chronic hepatitis. The 11 metastatic patients were seronegative for both HBsAg and HCV antibodies. They all had normal liver function and were histologically diagnosed as non-fibrotic livers. The resected non-tumorous liver specimens were taken as far from the tumor as possible, soaked in RNAlater solution (Ambion), and then stored at -80°C until use. Written informed consent was obtained from all patients according to a protocol approved by the Institutional Research Board of Osaka University Hospital.

Mice. *Mdm2*$^{fl/fl}$ mice were provided by Guillermina Lozano (University of Texas MD Anderson Cancer Center, Houston, Texas, USA) (15). Hepatocyte-specific Mdm2-knockout mice (*Mdm2*$^{fl/fl}$*alb-cre*) were generated by mating of *Mdm2*$^{fl/fl}$ mice and Alb-Cre transgenic mice (16, 21). *Trp53*$^{fl/fl}$ mice and ROSA26-LacZ mice were purchased from The Jackson Laboratory. Hepatocyte-specific Trp53-knockout mice (*Trp53*$^{fl/fl}$*alb-cre*) were generated by mating *Trp53*$^{fl/fl}$ mice and *alb-cre* transgenic mice. Hepatocyte-specific Mdm2- and Trp53-double-knockout mice (*Mdm2*$^{fl/fl}$*Trp53*$^{fl/fl}$*alb-cre*) were generated by mating *Mdm2*$^{fl/fl}$*Trp53*$^{fl/+}$ mice and *Mdm2*$^{fl/fl}$*Trp53*$^{fl/+}$*alb-cre* mice. Genomic recombination of the *Mdm2* and *Trp53* genes occurred at a rate of about 75% in the entire liver (data not shown). C57BL/6J mice and BALB/c mice were purchased from Charles River Laboratories Japan. They were maintained in a specific pathogen-free facility and treated with humane care with approval from the Animal Care and Use Committee of Osaka University Medical School.

Isolation and culture of murine hepatocytes and NPCs. Hepatocytes and NPCs were isolated from *Mdm2*$^{fl/fl}$ mice and *Mdm2*$^{fl/fl}$*alb-cre* mice by 2-step collagenase-pronase perfusion of mouse livers as previously described (17). Isolated hepatocytes were maintained at 37°C under 5% CO_2 in William's Eagle medium containing 10% FCS (Sigma-Aldrich), 100 nM dexamethasone, 100 nM insulin (Sigma-Aldrich) and L-glutamine (Invitrogen).

Histological analyses. The liver sections were stained with H&E. For detection of apoptotic cells, the liver sections were also subjected to TUNEL staining, according to a previously reported procedure (36). To assess their regenerative status, we stained liver sections for nuclear BrdU incorporation as previously described (59). To assess fibrosis, we stained the liver sections with picrosirius red. The percentage of collagen deposition was quantified using image analysis software (WinROOF visual system, Mitani Corp.) (59). For immunohistochemical detection of p53, α-SMA, cleaved caspase-3, and CTGF, the liver sections were respectively incubated with polyclonal rabbit anti-p53 antibody (Vector Laboratories Inc.), polyclonal rabbit anti-α-SMA antibody (Santa Cruz Biotechnology Inc.), polyclonal rabbit anti-cleaved caspase-3 antibody (Cell Signaling Technology Inc.), and polyclonal goat anti-CTGF antibody (Santa Cruz Biotechnology Inc.).

Senescence-associated β-galactosidase assay. To assess hepatocyte senescence, we performed a senescence-associated β-galactosidase assay according to a previously described procedure (60). Briefly, the frozen liver sections were fixed in 0.25% glutaraldehyde for 10 minutes and immersed overnight in SA-β-gal staining solution (0.5 mg/ml X-gal, 3 mM potassium ferricyanide, 3 mM potassium ferrocyanide, 2 mM $MgCl_2$, 0.25% Triton X-100, 0.1 M phosphate buffer, pH 6.0).

Determination of liver hydroxyproline content. Hydroxyproline content was determined essentially as described previously (59). Results are expressed as micrograms of hydroxyproline per gram of wet liver.

Western blot analysis. Liver tissue was lysed in lysis buffer (1% Nonidet P-40, 0.5% sodium deoxycholate, 0.1% sodium dodecyl sulfate, 1× protease inhibitor cocktail [Nacalai tesque], 1× phosphatase inhibitor cocktail [Nacalai tesque], phosphate-buffered saline, pH 7.4). The liver lysates were cleared by centrifugation at 10,000 *g* at 4°C for 15 minutes. The protein concentrations were determined using a bicinchoninic acid protein assay kit (Pierce). Equal amounts of protein lysates were electrophoretically separated by SDS polyacrylamide gels and transferred onto a polyvinylidene fluoride membrane. For immunodetection, the following antibodies were used: rabbit monoclonal antibody to p53, rabbit polyclonal antibody to Bax (Cell Signaling Technology), rabbit polyclonal antibody to p21, goat polyclonal antibody to CTGF, rabbit polyclonal antibody to p53 (Santa Cruz Biotechnology Inc.), rabbit polyclonal antibody to Noxa and p21 (Abcam), rabbit polyclonal antibody to Puma (ProSci Inc.), and mouse monoclonal antibody to β-actin (Sigma-Aldrich).

Real-time RT-PCR for mRNA. Total RNA extracted from cell lines and liver tissues using the RNeasy Mini Kit (QIAGEN) was reverse transcribed and subjected to real-time RT-PCR as previously described (59). mRNA expression of the specific genes was quantified using TaqMan Gene Expression Assays (Applied Biosystems) as follows: murine Col1a1 (assay ID: Mm00801666_g1), murine Col1a2 (Mm01165187_m1), murine Ctgf (Mm01192933_g1), murine Pmaip1 (Mm00451763_m1), murine Cdkn1a (Mm01303209_m1), murine Bax (Mm0043205_m1), murine Trp53 (Mm01731287_m1), murine Tgfb1 (Mm01178820_m1), murine Pdgfb (Mm01298578_m1), murine Mmp2 (Mm00439506_m1), murine Mmp14 (Mm01318969_g1), murine Timp1 (Mm01341361_m1), murine Acta2 (Mm01546133_m1), murine miR-17-92 (Mm03307063_pri), murine Actb (Mm02619580_g1), human COL1A1 (Hs01076777_m1), human CTGF (Hs00170014_m1), human PMAIP1 (Hs00560402_m1), human CDKN1A (Hs00355782_m1), human TP53 (Hs01034249_m1), human TGFB1 (Hs00998133_m1), human PDGFB (Hs00234042_m1), human BBC3 (Hs00248075_m1), human

BAX (Hs00180269_m1), and human ACTB (Hs99999903_m1). Human pri-miR-17-92 expression was quantified using the primers described previously (54). Transcript levels are presented as fold change.

Caspase-3/7 activity. Serum caspase-3/7 activity was measured with a luminescence substrate assay for caspase-3 and caspase-7 (Caspase-Glo assay, Promega) as described previously (61).

Real-time RT-PCR assays for mature miRNA. Total RNA including the miRNA fraction extracted from cell lines using the miRNeasy Mini Kit (QIAGEN) was reverse transcribed. Quantitative PCR was performed with TaqMan MicroRNA Assays (Applied Biosystems) specific for *miR-18a* (assay ID: 002422), *miR-19a* (assay ID: 000395), and *miR-19b* (assay ID: 000396). To normalize the expression levels of miRNAs, we used the TaqMan MicroRNA Assay specific for RNU6B (assay ID: 001093) as the endogenous control. Transcript levels are presented as fold change.

Transfections with miRNA. HepG2 cells were transfected with 10 nM Pre-miR miRNA precursor molecules (Ambion) of *MIR18A* (PM12973), *MIR19A* (PM10649), and *MIR19B* (PM10629) using RNAiMAX (Invitrogen) according to the manufacturer's instructions. Pre-miR negative control (Ambion) was used as a control.

Transfections with antisense of miRNA. HepG2 cells were transfected with 100 nM Anti-miR miRNA inhibitor (Ambion) of *MIR18A* (AM12973), *MIR19A* (AM10649) and *MIR19B* (AM10629) using RNAiMAX (Invitrogen) according to the manufacturer's instructions. Anti-miR negative control (Ambion) was used as a control.

Dual luciferase reporter assay. Plasmid pTS-589, which contains the *CTGF* promoter linked to the upstream of a firefly luciferase reporter gene (29), was transfected into HepG2 cells together with pRL-TK (Promega) using Lipofectamine LTX (Invitrogen). Upon 24 hours of Nutlin-3a (20 μM) or recombinant TGF-β (10 ng/ml) treatment, firefly luciferase activity was measured using the Luciferase Assay System (Promega) and normalized to *Renilla* luciferase activity.

siRNA-mediated knockdown. HepG2 cells were transfected with siRNA against *TP53* (Validated Stealth RNAi siRNA, oligo ID: VHS40367) (Invitrogen) using Lipofectamine RNAi-MAX (Invitrogen) according to the manufacturer's protocol. Stealth RNAi Negative Control Low GC (Invitrogen) was used as the control.

Isolation and culture of mouse HSCs. HSCs were isolated from C57BL/6J mice by 2-step collagenase-pronase perfusion of mouse liver, followed by density gradient centrifugation with 8.2% Nycodenz (Sigma-Aldrich) as previously described (59). Isolated HSCs were maintained at 37°C under 5% CO_2 in DMEM containing 10% FCS (Sigma-Aldrich). HSCs after a few passages were used for the experiments.

Generation of apoptotic body and coculture experiment with HSCs. Apoptotic bodies of hepatocytes were generated as described previously (50). Briefly, BNL CL.2 cells were UV irradiated (100 mJ/cm²) and incubated for 2 days in DMEM with 10% FCS. Next, floating apoptotic bodies were collected and centrifuged at 1,500 *g* for 5 minutes. HSCs (1.0×10^5) were starved for 48 hours in DMEM without FCS and then cocultured with apoptotic bodies (4.0×10^5) in DMEM with 10% FCS for the indicated time courses with or without 100 ng/ml recombinant CTGF (EMP Genetech).

Experimental protocol for ABT-737 administration. ABT-737, provided by Abbott Laboratories, was dissolved with a mixture of 30% propylene glycol, 5% Tween 80, and 65% D5W (5% dextrose in water), to a final pH of 4–5 as described previously (21). ABT-737 (100 mg/kg) was intraperitoneally administered to C57BL/6J mice, and 2 days later they were sacrificed for the various analyses.

Experimental protocol for ATH diet feeding. C57BL/6J mice, *Trp53*$^{fl/fl}$ mice, and *Trp53*$^{fl/fl}$*alb-cre* mice were subdivided into two groups: (a) mice fed an ATH diet (1.25% [w/w] cholesterol, 0.5% [w/w] cholic acid, and 16% [w/w] fat) for 4 weeks and (b) mice given standard chow (CRF-1, Charles River Laboratories Japan) for 4 weeks. After having been fasted for 8 hours, the animals were sacrificed for the various analyses.

Experimental protocol for TAA intraperitoneal administration. TAA (200 mg/kg) (Sigma-Aldrich) was intraperitoneally administered to *Trp53*$^{fl/fl}$ mice and *Trp53*$^{fl/fl}$*alb-cre* mice 3 times per week for 6 weeks, and then the animals were sacrificed for the various analyses.

Experimental protocol for hydrodynamic injection of p53 expression plasmid. BALB/c mice were given injection of pORF9-mp53 plasmid, an expression vector containing the murine p53 open reading frame (Invivogen) or its control plasmid via the tail vein by a hydrodynamic injection procedure (28) and sacrificed 2 days later for the various analyses.

Statistics. Data are expressed as median and interquartile range or mean ± SD. Statistical analyses were performed by the unpaired Mann-Whitney *U* test or 1-way ANOVA unless otherwise indicated. When ANOVA analyses were applied, differences in the mean values among the groups were examined by Scheffe post hoc correction. Correlations were assessed using the Pearson product-moment correlation coefficient. *P* values less than 0.05 were considered statistically significant.

Acknowledgments

We thank Guillermina Lozano (University of Texas MD Anderson Cancer Center) for providing the floxed *Mdm2* mice. We also thank Abbott Laboratories for providing ABT-737. We thank Kanako Mori for help with experiments.

Received for publication August 31, 2010, and accepted in revised form May 12, 2011.

Address correspondence to: Tetsuo Takehara, Department of Gastroenterology and Hepatology, Osaka University Graduate School of Medicine, 2-2 Yamada-oka, Suita, Osaka 565-0871, Japan. Phone: 81.6.6879.3621; Fax: 81.6.6879.3629; E-mail: takehara@gh.med.osaka-u.ac.jp.

1. Vousden KH, Lu X. Live or let die: the cell's response to p53. *Nat Rev Cancer.* 2002;2(8):594–604.
2. Bensaad K, et al. TIGAR, a p53-inducible regulator of glycolysis and apoptosis. *Cell.* 2006;126(1):107–120.
3. Hu W, Zhang C, Wu R, Sun Y, Levine A, Feng Z. Glutaminase 2, a novel p53 target gene regulating energy metabolism and antioxidant function. *Proc Natl Acad Sci U S A.* 2010;107(16):7455–7460.
4. Crighton D, et al. DRAM, a p53-induced modulator of autophagy, is critical for apoptosis. *Cell.* 2006;126(1):121–134.
5. Tyner SD, et al. p53 mutant mice that display early ageing-associated phenotypes. *Nature.* 2002; 415(6867):45–53.
6. Minamino T, et al. A crucial role for adipose tissue p53 in the regulation of insulin resistance. *Nat Med.* 2009; 15(9):1082–1087.
7. Sano M, et al. p53-induced inhibition of Hif-1 causes cardiac dysfunction during pressure overload. *Nature.* 2007;446(7134):444–448.
8. Akyol G, et al. P53 and proliferating cell nuclear antigen (PCNA) expression in non-tumoral liver diseases. *Pathol Int.* 1999;49(3):214–221.
9. Panasiuk A, Dzieciol J, Panasiuk B, Prokopowicz D. Expression of p53, Bax and Bcl-2 proteins in hepatocytes in non-alcoholic fatty liver disease. *World J Gastroenterol.* 2006;12(38):6198–6202.
10. Attallah AM, Shiha GE, Ismail H, Mansy SE, El-Sherbiny R, El-Dosoky I. Expression of p53 protein in liver and sera of patients with liver fibrosis, liver cirrhosis or hepatocellular carcinoma associated with chronic HCV infection. *Clin Biochem.* 2009;42(6):455–461.
11. Loguercio C, et al. Liver p53 expression in patients with HCV-related chronic hepatitis. *J Viral Hepat.* 2003;10(4):266–270.
12. Papakyriakou P, et al. Apoptosis and apoptosis related proteins in chronic viral liver disease. *Apoptosis.* 2002;7(2):133–141.
13. Kruse JP, Gu W. Modes of p53 regulation. *Cell.* 2009;137(4):609–622.
14. Gressner OA, Gressner AM. Connective tissue growth factor: a fibrogenic master switch in fibrotic liver diseases. *Liver Int.* 2008;28(8):1065–1079.
15. Grier JD, Xiong S, Elizondo-Fraire AC, Parant JM, Lozano G. Tissue-specific differences of p53 inhibition by Mdm2 and Mdm4. *Mol Cell Biol.* 2006;26(1):192–198.
16. Takehara T, et al. Hepatocyte-specific disruption of Bcl-xL leads to continuous hepatocyte apoptosis and liver fibrotic responses. *Gastroenterology.*

2004;127(4):1189–1197.
17. Sakamori R, et al. Signal transducer and activator of transcription 3 signaling within hepatocytes attenuates systemic inflammatory response and lethality in septic mice. *Hepatology*. 2007;46(5):1564–1573.
18. Vassilev LT, et al. In vivo activation of the p53 pathway by small-molecule antagonists of MDM2. *Science*. 2004;303(5659):844–848.
19. Bataller R, Brenner DA. Liver fibrosis. *J Clin Invest*. 2005;115(2):209–218.
20. Friedman SL. Mechanisms of hepatic fibrogenesis. *Gastroenterology*. 2008;134(6):1655–1669.
21. Hikita H, et al. BH3-only protein bid participates in the Bcl-2 network in healthy liver cells. *Hepatology*. 2009;50(6):1972–1980.
22. Hikita H, et al. The Bcl-xL inhibitor, ABT-737, efficiently induces apoptosis and suppresses growth of hepatoma cells in combination with sorafenib. *Hepatology*. 2010;52(4):1310–1321.
23. Mitchell C, Willenbring H. A reproducible and well-tolerated method for 2/3 partial hepatectomy in mice. *Nat Protoc*. 2008;3(7):1167–1170.
24. Larter CZ, Yeh MM. Animal models of NASH: getting both pathology and metabolic context right. *J Gastroenterol Hepatol*. 2008;23(11):1635–1648.
25. Matsuzawa N, et al. Lipid-induced oxidative stress causes steatohepatitis in mice fed an atherogenic diet. *Hepatology*. 2007;46(5):1392–1403.
26. Safadi R, et al. Immune stimulation of hepatic fibrogenesis by CD8 cells and attenuation by transgenic interleukin-10 from hepatocytes. *Gastroenterology*. 2004;127(3):870–882.
27. Lin Y, et al. Tumour suppressor p53 and Rb genes in human hepatocellular carcinoma. *Ann Acad Med Singapore*. 1996;25(1):22–30.
28. Suzuki T, et al. Intravenous injection of naked plasmid DNA encoding hepatitis B virus (HBV) produces HBV and induces humoral immune response in mice. *Biochem Biophys Res Commun*. 2003; 300(3):784–788.
29. Eguchi T, et al. Regulatory mechanism of human connective tissue growth factor (CTGF/Hcs24) gene expression in a human chondrocytic cell line, HCS-2/8. *J Biochem*. 2001;130(1):79–87.
30. Cicha I, Goppelt-Struebe M. Connective tissue growth factor: context-dependent functions and mechanisms of regulation. *Biofactors*. 2009; 35(2):200–208.
31. Dews M, et al. Augmentation of tumor angiogenesis by a Myc-activated microRNA cluster. *Nat Genet*. 2006; 38(9):1060–1065.
32. Ernst A, et al. De-repression of CTGF via the miR-17-92 cluster upon differentiation of human glioblastoma spheroid cultures. *Oncogene*. 2010; 29(23):3411–3422.
33. Tanzer A, Stadler PF. Molecular evolution of a microRNA cluster. *J Mol Biol*. 2004;339(2):327–335.
34. Montes de Oca Luna R, Wagner DS, Lozano G. Rescue of early embryonic lethality in mdm2-deficient mice by deletion of p53. *Nature*. 1995; 378(6553):203–206.
35. Xiong S, Van Pelt CS, Elizondo-Fraire AC, Liu G, Lozano G. Synergistic roles of Mdm2 and Mdm4 for p53 inhibition in central nervous system development. *Proc Natl Acad Sci U S A*. 2006;103(9):3226–3231.
36. Hikita H, et al. Mcl-1 and Bcl-xL cooperatively maintain integrity of hepatocytes in developing and adult murine liver. *Hepatology*. 2009;50(4):1217–1226.
37. Brigstock DR. The connective tissue growth factor/cysteine-rich 61/nephroblastoma overexpressed (CCN) family. *Endocr Rev*. 1999;20(2):189–206.
38. Gao R, Brigstock DR. A novel integrin alpha5beta1 binding domain in module 4 of connective tissue growth factor (CCN2/CTGF) promotes adhesion and migration of activated pancreatic stellate cells. *Gut*. 2006;55(6):856–862.
39. Song JJ, et al. Connective tissue growth factor (CTGF) acts as a downstream mediator of TGF-beta1 to induce mesenchymal cell condensation. *J Cell Physiol*. 2007;210(2):398–410.
40. Abou-Shady M, et al. Connective tissue growth factor in human liver cirrhosis. *Liver*. 2000;20(4):296–304.
41. Hora C, et al. Connective tissue growth factor, steatosis and fibrosis in patients with chronic hepatitis C. *Liver Int*. 2008;28(3):370–376.
42. Williams EJ, Gaca MD, Brigstock DR, Arthur MJ, Benyon RC. Increased expression of connective tissue growth factor in fibrotic human liver and in activated hepatic stellate cells. *J Hepatol*. 2000;32(5):754–761.
43. Paradis V, et al. High glucose and hyperinsulinemia stimulate connective tissue growth factor expression: a potential mechanism involved in progression to fibrosis in nonalcoholic steatohepatitis. *Hepatology*. 2001;34(4 pt 1):738–744.
44. George J, Tsutsumi M. siRNA-mediated knockdown of connective tissue growth factor prevents N-nitrosodimethylamine-induced hepatic fibrosis in rats. *Gene Ther*. 2007;14(10):790–803.
45. Li G, et al. Inhibition of connective tissue growth factor by siRNA prevents liver fibrosis in rats. *J Gene Med*. 2006;8(7):889–900.
46. Paradis V, et al. Expression of connective tissue growth factor in experimental rat and human liver fibrosis. *Hepatology*. 1999;30(4):968–976.
47. Gressner OA, Lahme B, Demirci I, Gressner AM, Weiskirchen R. Differential effects of TGF-beta on connective tissue growth factor (CTGF/CCN2) expression in hepatic stellate cells and hepatocytes. *J Hepatol*. 2007;47(5):699–710.
48. Weng HL, et al. Profibrogenic transforming growth factor-beta/activin receptor-like kinase 5 signaling via connective tissue growth factor expression in hepatocytes. *Hepatology*. 2007;46(4):1257–1270.
49. Tong Z, Chen R, Alt DS, Kemper S, Perbal B, Brigstock DR. Susceptibility to liver fibrosis in mice expressing a connective tissue growth factor transgene in hepatocytes. *Hepatology*. 2009;50(3):939–947.
50. Canbay A, Taimr P, Torok N, Higuchi H, Friedman S, Gores GJ. Apoptotic body engulfment by a human stellate cell line is profibrogenic. *Lab Invest*. 2003;83(5):655–663.
51. Ku JL, et al. Establishment and characterisation of six human biliary tract cancer cell lines. *Br J Cancer*. 2002;87(2):187–193.
52. Ohgawara T, et al. Regulation of chondrocytic phenotype by micro RNA 18a: involvement of Ccn2/Ctgf as a major target gene. *FEBS Lett*. 2009; 583(6):1006–1010.
53. Duisters RF, et al. miR-133 and miR-30 regulate connective tissue growth factor: implications for a role of microRNAs in myocardial matrix remodeling. *Circ Res*. 2009;104(2):170–178.
54. Yan HL, et al. Repression of the miR-17-92 cluster by p53 has an important function in hypoxia-induced apoptosis. *EMBO J*. 2009;28(18):2719–2732.
55. Komarov PG, et al. A chemical inhibitor of p53 that protects mice from the side effects of cancer therapy. *Science*. 1999;285(5434):1733–1737.
56. Ostrau C, et al. Lovastatin attenuates ionizing radiation-induced normal tissue damage in vivo. *Radiother Oncol*. 2009;92(3):492–499.
57. Vozenin-Brotons MC, et al. Fibrogenic signals in patients with radiation enteritis are associated with increased connective tissue growth factor expression. *Int J Radiat Oncol Biol Phys*. 2003;56(2):561–572.
58. Haydont V, Riser BL, Aigueperse J, Vozenin-Brotons MC. Specific signals involved in the long-term maintenance of radiation-induced fibrogenic differentiation: a role for CCN2 and low concentration of TGF-beta1. *Am J Physiol Cell Physiol*. 2008;294(6):C1332–C1341.
59. Kodama T, et al. Thrombocytopenia exacerbates cholestasis-induced liver fibrosis in mice. *Gastroenterology*. 2010;138(7):2487–2498.
60. Itahana K, Campisi J, Dimri GP. Methods to detect biomarkers of cellular senescence: the senescence-associated beta-galactosidase assay. *Methods Mol Biol*. 2007;371:21–31.
61. Kodama T, et al. BH3-only activator proteins, Bid and Bim, are dispensable for Bak/Bax-dependent thrombocyte apoptosis induced by Bcl-xL deficiency: molecular requisites for the mitochondrial pathway to apoptosis in platelets. *J Biol Chem*. 2011;286(16):13905–13913.

GASTROENTEROLOGY 2010;138:2487–2498

Thrombocytopenia Exacerbates Cholestasis-Induced Liver Fibrosis in Mice

TAKAHIRO KODAMA,* TETSUO TAKEHARA,* HAYATO HIKITA,* SATOSHI SHIMIZU,* WEI LI,* TAKUYA MIYAGI,* ATSUSHI HOSUI,* TOMOHIDE TATSUMI,* HISASHI ISHIDA,* SEIJI TADOKORO,‡ AKIO IDO,§ HIROHITO TSUBOUCHI,§ and NORIO HAYASHI*

*Department of Gastroenterology and Hepatology and ‡Department of Hematology and Oncology, Osaka University Graduate School of Medicine, Suita, Osaka; and §Digestive Disease and Life-style Related Disease Health Research, Human and Environmental Science, Kagoshima University Graduate School of Medical and Dental Science, Kagoshima, Kagoshima, Japan

BACKGROUND & AIMS: Circulating platelet counts gradually decrease in parallel with progression of chronic liver disease. Thrombocytopenia is a common complication of advanced liver fibrosis and is thought to be a consequence of the destruction of circulating platelets that occurs during secondary portal hypertension or hypersplenism. It is not clear whether thrombocytopenia itself affects liver fibrosis. **METHODS:** Thrombocytopenic mice were generated by disruption of *Bcl-xL*, which regulates platelet life span, specifically in thrombocytes. Liver fibrosis was examined in thrombocytopenic mice upon bile duct ligation. Effect of platelets on hepatic stellate cells (HSCs) was investigated in vitro. **RESULTS:** Thrombocytopenic mice developed exacerbated liver fibrosis, with increased expression of type I collagen $\alpha 1$ and $\alpha 2$, during cholestasis. In vitro experiments revealed that, upon exposure to HSCs, platelets became activated, released hepatocyte growth factor (HGF), and then inhibited HSC expression of the type I collagen genes in a Met signal-dependent manner. In contrast to the wild-type mice, the thrombocytopenic mice did not accumulate hepatic platelets or phosphorylate Met in the liver following bile duct ligation. Administration of recombinant HGF to thrombocytopenic mice reduced liver fibrosis to the levels observed in wild-type mice and attenuated hepatic expression of the type I collagen genes. **CONCLUSIONS: Thrombocytopenia exacerbates liver fibrosis; platelets have a previously unrecognized, antifibrotic role in suppressing type I collagen expression via the HGF-Met signaling pathway.**

Keywords: Bcl-2; Apoptosis; Cre; Conditional Knockout.

Cirrhosis followed by chronic liver disease is considered to be a major medical issue worldwide, causing significant morbidity and mortality because it can progress to liver failure or develop into hepatocellular caricinoma. The pathogenesis of cirrhosis is characterized by liver fibrosis, which is defined as excessive production and deposition of several extracellular matrix (ECM) proteins. The accumulation of ECM proteins, as fibrotic scars, gradually distorts liver structure and increases intrahepatic resistance to blood flow, leading to portal hypertension.[1] Among the deposited ECM proteins in the cirrhotic liver, type I collagen is the most prevalent, and it is well known that activated hepatic stellate cells (HSCs) are major collagen-producing cells.[1,2] With fibrosis progression in chronic liver disease, patients often suffer from thrombocytopenia, which promotes a tendency for bleeding and can result in mortal hemorrhagic complications such as variceal bleeding.[3] Multiple factors have been proposed for the pathogenesis of thrombocytopenia in advanced liver fibrosis; they include enhanced destruction of circulating platelets in an enlarged spleen arising because of portal hypertension[4] and reduced production of thrombopoietin (TPO) in the liver.[3] In general, concomitant thrombocytopenia is considered to be a secondary phenomenon caused by liver fibrosis progression. However, whether thrombocytopenia per se affects liver fibrosis has not been thoroughly examined. In the present study, we generated a novel mouse model of severe thrombocytopenia by thrombocyte-specific knockout of Bcl-xL, a critical regulator of thrombocyte life span,[5] and found that the mice developed exacerbated liver fibrosis during bile duct ligation (BDL)-induced cholestasis because of an increase in type I collagen gene expression. In vitro study revealed that platelets negatively regulated type I collagen gene expression in activated HSCs via a pathway involving the platelet-derived hepatocyte growth factor (HGF) and its receptor, Met.

Abbreviations used in this paper: ALP, alkaline phosphatase; α-SMA, α-smooth muscle actin; BDL, bile duct ligation; BrdU, 5-bromo-2-deoxyuridine; ECM, extracellular matrix; HGF, hepatocyte growth factor; HSCs, hepatic stellate cells; MMP, matrix metalloprotease; mRNA, messenger RNA; Pf4, platelet factor 4; siRNA, small interfering RNA; T-Bil, total bilirubin; TPO, thrombopoietin; TUNEL, terminal deoxynucleotidyl transferase-mediated deoxyuridine triphosphate nick-end labeling.

0016-5085/$36.00
doi:10.1053/j.gastro.2010.02.054

Materials and Methods

Mice

Thrombocyte-specific Bcl-xL knockout mice (*bcl-x$^{flox/flox}$ Pf4-Cre*) were generated by mating *bcl-x$^{flox/flox}$* mice[6,7] and *Pf4-Cre* transgenic mice.[8] They were maintained in a specific pathogen-free facility and treated with humane care under approval from the Animal Care and Use Committee of Osaka University Medical School.

BDL Treatment

Wild-type (*bcl-x$^{fl/fl}$*) and knockout (*bcl-x$^{fl/fl}$ Pf4-Cre*) mice were subjected to BDL as previously reported.[9] Briefly, the common bile duct was ligated 3 times with 5-0 silk sutures and then cut between the ligatures. After 10 days, the animals were killed for the following analyses. For more detailed description of the Materials and Methods used, see the Supplementary Materials and Methods.

Results

Thrombocyte-Specific Disruption of Bcl-xL Causes Massive Thrombocytopenia

Previous research has demonstrated that traditional knockout mice lacking a single allele of the *bcl-x* gene develop mild thrombocytopenia.[5] We generated thrombocyte-specific Bcl-xL knockout mice by crossing *floxed bcl-x* mice[6,7] and *Pf4-Cre* transgenic mice.[8] After mating *bcl-x$^{flox/flox}$Pf4-Cre* mice with *bcl-x$^{flox/flox}$* mice, *bcl-x$^{flox/flox}$Pf4-Cre* mice were born at the expected Mendelian frequency and did not show any developmental abnormality. As expected, *bcl-x$^{flox/flox}$Pf4-Cre* mice showed severe thrombocytopenia without any phenotypes of other hematopoietic lineages (Figure 1*A*). Western blot analysis confirmed a substantial decrease in Bcl-xL expression in circulating platelets of *bcl-x$^{flox/flox}$Pf4-Cre* mice compared with *bcl-x$^{flox/flox}$* mice (Figure 1*B*). CD41 protein, a specific surface receptor expressed in the thrombocyte lineage,[10,11] was used as a loading control of platelets. To demonstrate the thrombocyte-lineage specificity of the Platelet factor 4 (Pf4) promotor that we used, we examined Bcl-xL protein expression in several tissues and hematopoietic cells of *bcl-x$^{flox/flox}$ Pf4-Cre* mice and *bcl-x$^{flox/flox}$* mice by Western blotting. In all of these tissues and cells, Bcl-xL protein expression was not different between the 2 groups (Figure 1*C*), indicating that the Pf4 promotor was specific to platelets and their precursors in our mice model. The physiologic liver status was not different between the 2 groups as evidenced by serum biochemistry data for alanine transaminase (ALT), total bilirubin (T-Bil), and alkaline phosphatase (ALP) (Figure 1*D*) as well as for liver histology (Figure 1*E*). In the following experiments, *bcl-x$^{flox/flox}$ Pf4-Cre* mice were crossed with *bcl-x$^{flox/flox}$* mice, and their offspring, *bcl-x$^{flox/flox}$ Pf4-Cre* mice and *bcl-x$^{flox/flox}$* mice, were used as thrombocytopenic mice and control littermates, respectively.

Thrombocytopenic Mice Display Exacerbation of Cholestasis-Induced Liver Fibrosis

To investigate the effect of thrombocytopenia on liver fibrosis, these mice were subjected to BDL, a well-established model of liver fibrosis,[9] and examined 10 days later. Cholestasis was similarly induced in both groups as evidenced by serum levels of alkaline phosphatase and T-Bil (Figure 2*A*). Both oncotic necrosis, also known as bile infarcts, and apoptosis are characteristic features of liver injury in the BDL model.[12] Although serum ALT levels were slightly lower in the thrombocytopenic mice than in the control littermates (Figure 2*A*), the area of oncotic necrosis as well as the number of terminal deoxynucleotidyl transferase-mediated deoxyuridine triphosphate nick-end labeling (TUNEL)-positive cells in the liver was not significantly different between the 2 groups (Figure 2*B*). The number of accumulating neutrophils, which are known to play a major role in liver inflammation induced by cholestasis,[12] did not differ between the 2 groups as assessed by chloroacetate esterase staining of the liver sections (Figure 2*C*). Similarly, the T lymphocyte and macrophage population in the liver did not differ between the 2 groups as determined by real-time reverse-transcription polymerase chain reaction (Supplementary Figure 1). Upon BDL treatment, compensatory regeneration occurred, but there was no significant difference between the 2 groups as determined by the count of 5-bromo-2-deoxyuridine (BrdU)-positive cells (Figure 2*D*).

To assess liver fibrosis, hepatic collagen deposition was evaluated by picrosirius red staining of liver sections. Collagen deposition increased following BDL treatment in both groups and was significantly higher in the thrombocytopenic mice than in the control littermates (Figure 2*E*). Similarly, the hepatic hydroxyproline content, a biochemical marker of collagen accumulation,[6] in the thrombocytopenic mice was elevated to a level significantly higher than in the control littermates (Figure 2*E*). The major form of collagen in cirrhosis is known to be type I collagen composed of 2 α1 and 1 α2 chains. After BDL, hepatic expression of type I collagen α1 and α2 genes, *col1a1* and *col1a2*, sharply rose in both groups and was significantly higher in the thrombocytopenic mice than in the control littermates (Figure 2*F*). Western blot analysis confirmed that the hepatic expression of type I collagen protein was higher in the thrombocytopenic mice than in the control littermates (Figure 2*F*). These results indicated that thrombocytopenia enhanced collagen synthesis in the liver and exacerbated liver fibrosis without affecting liver inflammation, apoptosis, and regeneration.

Platelets Become Activated and Inhibit Collagen Synthesis in Activated HSCs In Vitro

To explore the underlying mechanisms of increased collagen synthesis after BDL in the liver of the thrombocytopenic mice, we tested the hypothesis that

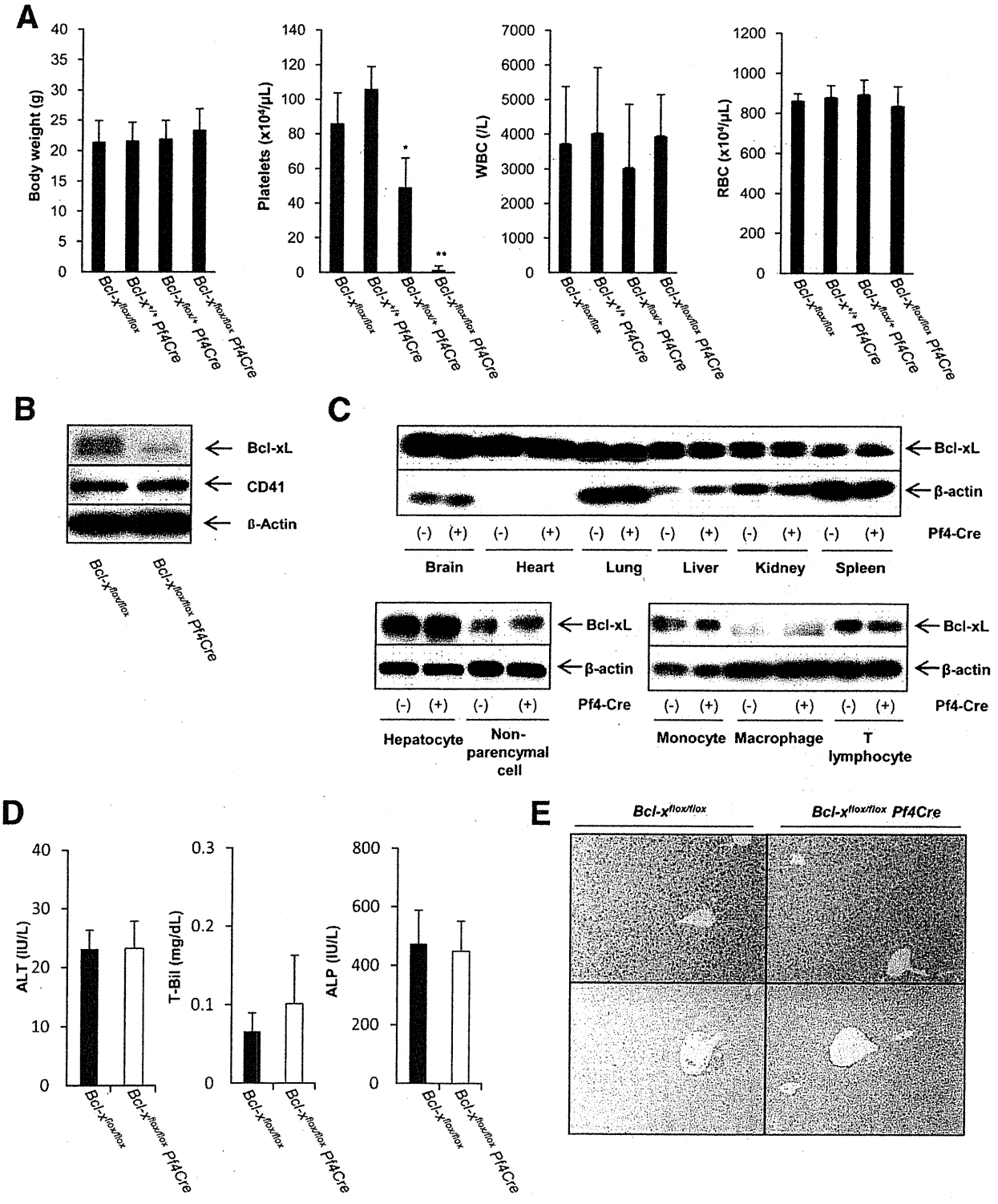

Figure 1. Thrombocyte-specific Bcl-xL knockout mice show massive thrombocytopenia. (*A*) Body weight and circulating blood cell counts of offspring from mating of *bcl-x*$^{flox/+}$ *Pf4-Cre* mice and *bcl-x*$^{flox/+}$ mice; 7–11 mice per group; **P* < .05 vs the other 3 groups, ***P* < .05 vs the other 3 groups. (*B*) Expression of Bcl-xL and CD41 protein in circulating platelets by Western blot analysis. β-Actin is included as a control. (*C*) Expression of Bcl-xL in indicated tissues and cells by Western blot analysis. Heart tissue lysates were equally loaded between the 2 groups confirmed by expression of glyceraldehyde-3-phosphate dehydrogenase, although the data are not shown. Pf4-Cre(+) and Pf4-Cre(−) stand for *bcl-x*$^{flox/flox}$ *Pf4-Cre* and *bcl-x*$^{flox/flox}$, respectively. (*D*) Serum levels of alanine aminotransferase (*ALT*), total bilirubin (*T-Bil*), and alkaline phosphatase (*ALP*). (*E*) H&E staining (*upper panel*) and picrosirius red staining (*lower panel*) of liver sections.

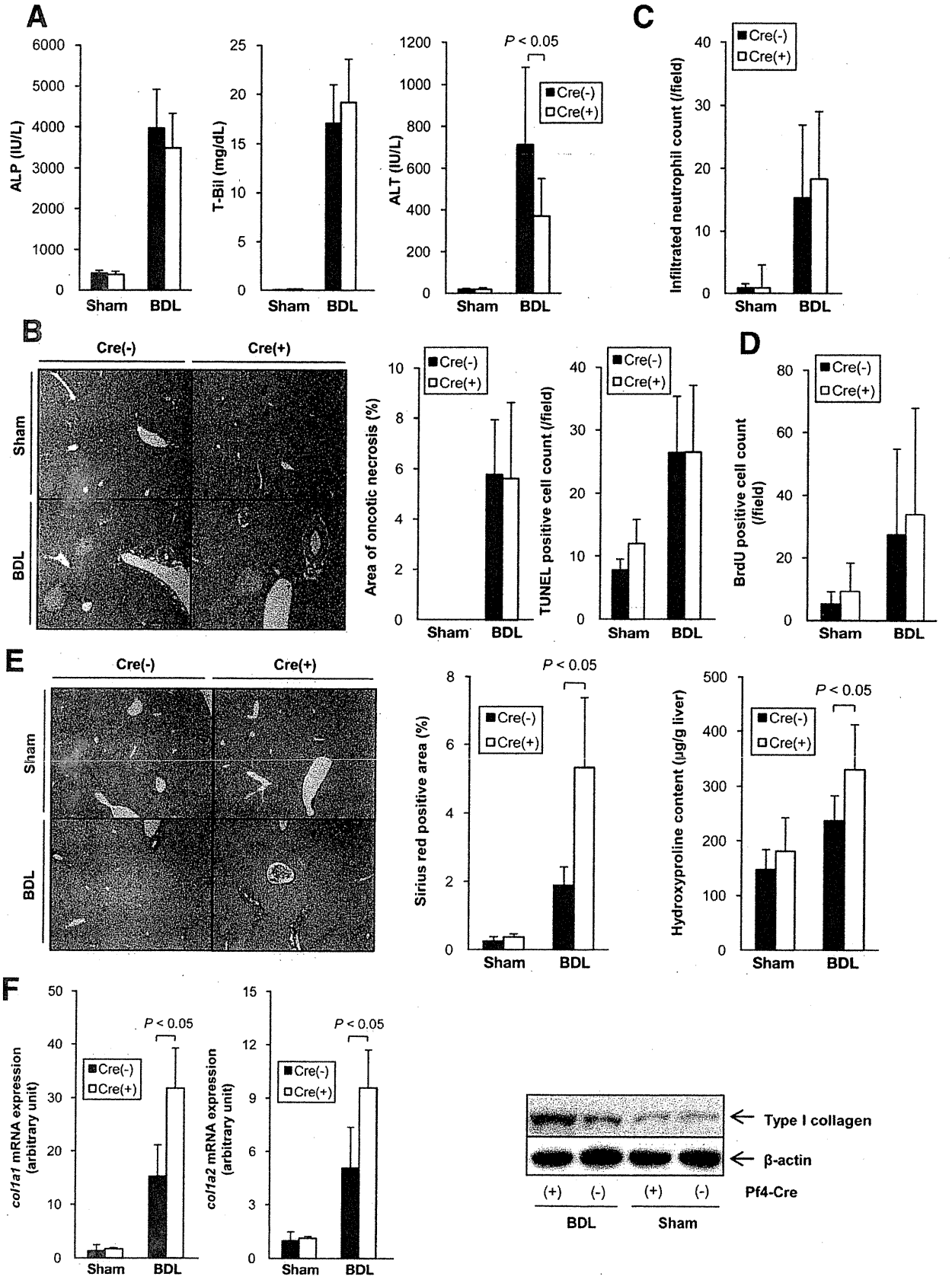

BASIC: LIVER, PANCREAS, AND BILIARY TRACT

platelets would suppress collagen production in activated HSCs, which are known as the main collagen-producing cells in the injured liver.[13] We isolated HSCs from C57BL/6J mice and cultured them for 7 to 10 days, leading to their transdifferentiation from quiescent cells to activated myofibroblast-like cells.[13] These culture-activated HSCs were then cocultured with platelets isolated from C57BL/6J mice. Expression of *col1a1* and *col1a2* messenger RNA (mRNA) in HSCs was clearly inhibited upon addition of platelets (Figure 3*A*). After a few passages, similar suppression of type I collagen gene expression was observed in these cells, appearing in a platelet dose-dependent manner (Figure 3*B*). Type I collagen protein in HSCs also decreased upon coculture with platelets as determined by Western blot analysis (Figure 3*C*). Platelets generally execute their biologic effects through activation that is associated with their shape change and granule secretion represented by P-selectin (CD62P) translocation from the α-granule to the outer surface.[14,15] To find whether or not platelets are activated upon exposure to HSCs, platelets from cocultures with HSCs were analyzed by flow cytometry, which revealed their dynamic shape change and the surface translocation of P-selectin (Figure 3*D*). The levels of soluble P-selectin, which are also known to reflect platelet activation,[15] were significantly higher in the coculture medium with platelets and HSCs than those in the medium with platelets alone (Figure 3*E*). These results demonstrated that platelets were activated upon exposure to HSCs and inhibited collagen synthesis in activated HSCs.

Soluble Factors Released From Activated Platelets Are Involved in the Inhibition of Collagen Synthesis in HSCs

Once activated, platelets are known to affect many other cells via secreted soluble factors or direct interaction with surface molecules. Platelet activation and secretion can be triggered artificially by a variety of strong agonists such as thrombin.[14] To examine whether soluble factors secreted from activated platelets are involved in the suppression of collagen synthesis in HSCs, we stimulated platelets with or without thrombin and applied the supernatant to HSCs. Thrombin induced clear platelet activation as evidenced by shape changes and P-selectin translocation (Figure 4*A*). The levels of soluble P-selectin were also significantly higher in the supernatant of thrombin-stimulated platelets than in the supernatant of unstimulated platelets (Figure 4*B*). The supernatant of thrombin-stimulated platelets suppressed type I collagen gene expression in HSCs but that of unstimulated platelets did not (Figure 4*C*), indicating that soluble factors derived from activated platelets were involved in suppressing collagen production in HSCs.

HGF in Platelet Granules Contributes to the Inhibition of Collagen Synthesis in HSCs

To identify the platelet-derived soluble factors that contribute to the suppression of collagen synthesis in HSCs, we focused on HGF, a pleiotropic growth factor,[16,17] which is known to exist in platelets.[18] We hypothesized that, in our in vitro study, HGF may be secreted from activated platelets and inhibit collagen synthesis in HSCs. Administration of recombinant HGF to HSCs inhibited *col1a1* and *col1a2* gene expression (Figure 5*A*). Consecutively, murine platelets were capable of releasing HGF upon exposure to thrombin (Figure 5*B*). Importantly, the levels of HGF were significantly higher in the coculture supernatant of HSCs and platelets than in that of platelets alone (Figure 5*C*). We next examined whether HGF secreted from activated platelets is actually involved in suppressing collagen synthesis in HSCs. The multiple biologic activities of HGF are mediated by Met, a transmembrane tyrosine kinase receptor, which transduces the effects of HGF upon phosphorylation.[19] Western blot analysis showed that the Met protein of HSCs was phosphorylated at multiple sites after coculture with platelets (Figure 5*D*) and proteins of its downstream pathways such as Erk1/2, Akt, and stat3 were phosphorylated as well (Figure 5*D*). To assess the involvement of this activated signaling in the inhibition of collagen production in HSCs, we performed small interfering RNA (siRNA)-mediated knockdown of *met*. Transfection of *met* siRNA into HSCs resulted in a substantial decrease in Met expression (Figure 5*E*) and blunted HGF-induced suppression of type I collagen gene expression (Figure 5*F*). Under these conditions, *met* knockdown abolished platelet-induced suppression of type I collagen gene expression in HSCs (Figure 5*F*). This result clearly demonstrated that HGF/Met signaling was indispensable for platelet-mediated inhibition of the collagen synthesis in activated HSCs.

Figure 2. Thrombocytopenic mice show exacerbated liver fibrosis following BDL treatment. *bcl-x$^{flox/flox}$ Pf4-Cre* mice and *bcl-x$^{flox/flox}$* mice were sham operated or subjected to BDL and analyzed 10 days later (8–12 mice per group). Cre(+) and Cre(−) stand for *bcl-x$^{flox/flox}$ Pf4-Cre* and *bcl-x$^{flox/flox}$*, respectively. (*A*) Serum levels of alkaline phosphatase (*ALP*), total bilirubin (*T-Bil*), and alanine aminotransferase (*ALT*). (*B*) Oncotic necrosis and hepatocyte apoptosis were evaluated by H&E staining and TUNEL staining of liver sections, respectively. (*C*) Infiltrated neutrophil count was evaluated by chloroacetate esterase staining of liver sections. (*D*) Liver regeneration was evaluated by 5-bromo-2-deoxyuridine (*BrdU*) staining of liver sections. (*E*) Liver fibrosis was evaluated by picrosirius red staining of liver sections and total liver hydroxyproline levels. (*F*) *co1a1* And *col1a2* mRNA levels in the liver were determined by real-time reverse-transcription polymerase chain reaction. Expression of type I collagen protein in the liver was assessed by Western blotting.

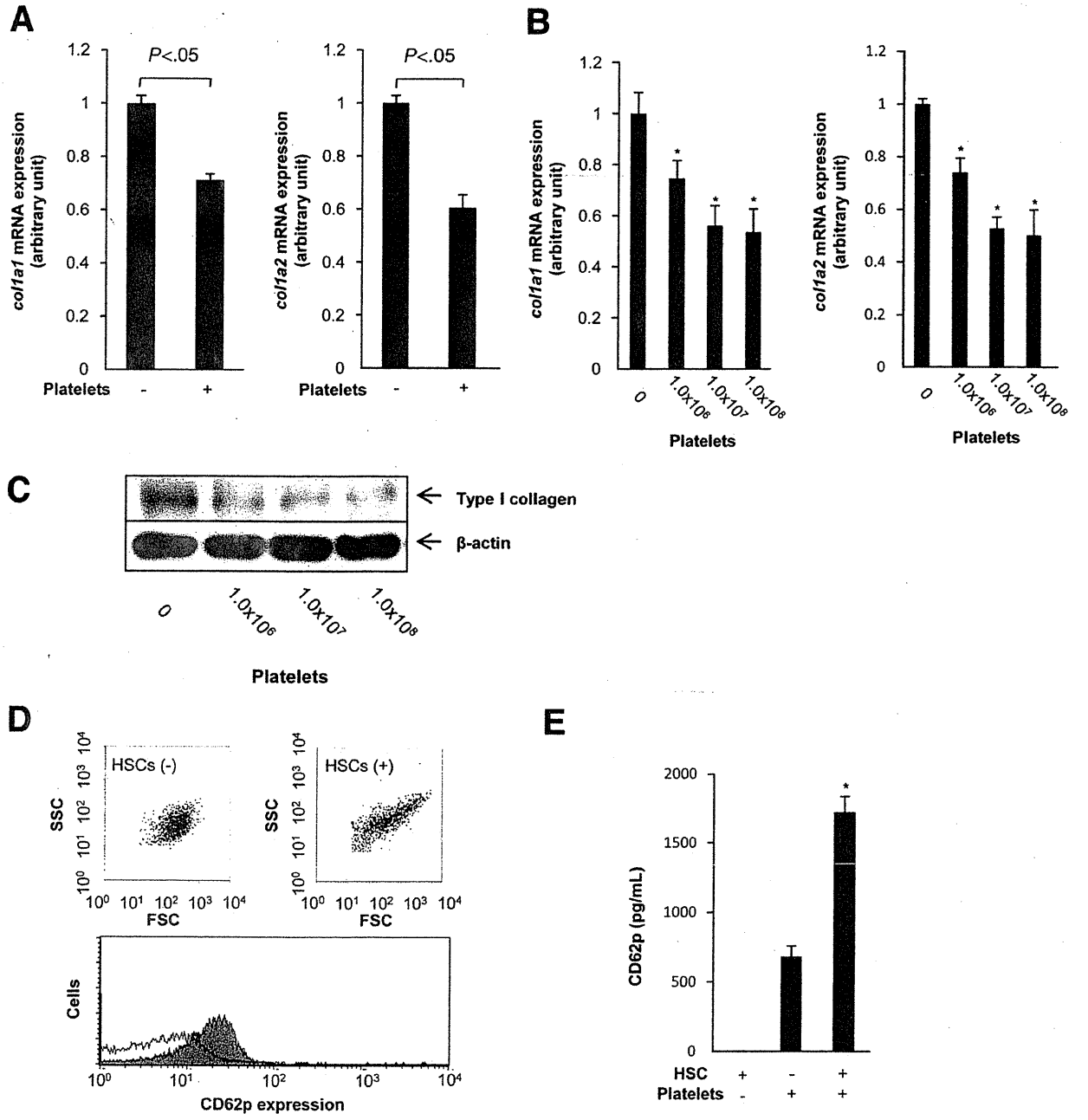

Figure 3. Platelets become activated and inhibit collagen synthesis in activated HSCs in vitro. (*A* and *B*) *col1a1* And *col1a2* mRNA levels in HSCs by real-time reverse-transcription polymerase chain reaction. Primary isolated HSCs were cocultured with 1.0×10^8 platelets for 6 hours (*A*), n = 3/group. HSCs (1.0×10^5) were cocultured with indicated dosages of platelets for 6 hours (*B*), n = 3/group, $^*P < .05$ vs HSCs with control group. (*C*) Expression of type I collagen protein in HSCs determined by Western blot analysis. HSCs (5.0×10^5) were cocultured with indicated dosages of platelets for 14 hours. (*D* and *E*) Activation of platelets on exposure to HSCs. Platelets (1.0×10^7) were cocultured with or without 1.0×10^5 HSCs for 1 hour. Shape change and P-selectin surface expression of platelets were analyzed by flow cytometry (*D*); representative data are shown; note that FSC increased with addition of HSCs; *closed histograms* and *open histograms* indicate P-selectin surface expression of platelets cocultured with or without HSCs, respectively. Soluble P-selectin levels of the culture supernatants were determined by ELISA (*E*), n = 3/group, $^*P < .05$ vs the other 2 groups.

HGF Administration Alleviates Liver Fibrosis in Thrombocytopenic Mice to the Level in the Control Littermates After BDL

To investigate the involvement of platelets in cholestasis-induced liver fibrosis in vivo, we examined platelet kinetics upon BDL treatment. To find whether platelets accumulate in the liver, we examined the expression of CD41 protein. Western blot analysis revealed that CD41 expression in the liver was up-regulated upon BDL treatment in the control littermates but not in the thrombocy-

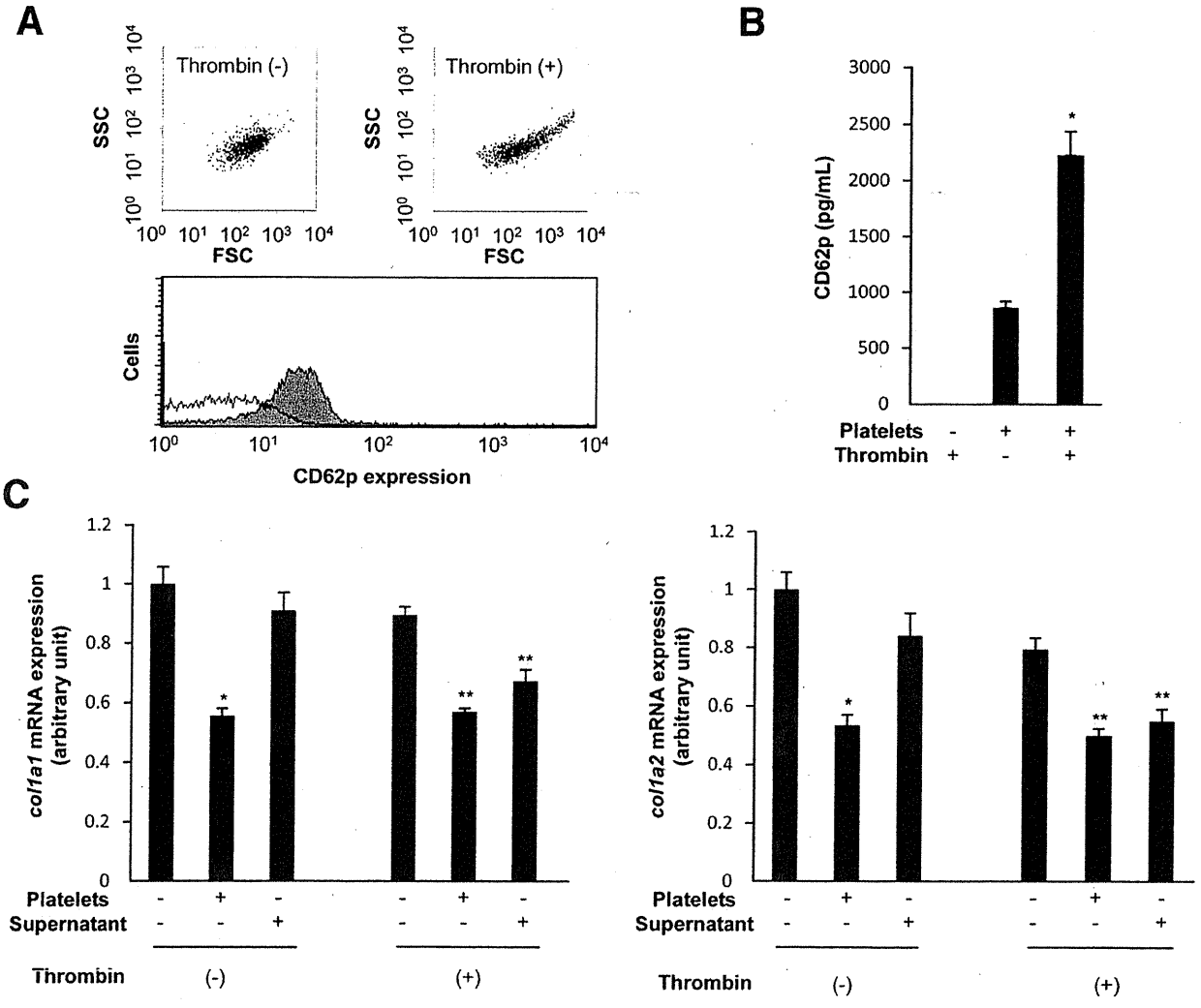

Figure 4. Soluble factors released from activated platelets are involved in the inhibition of collagen synthesis in HSCs. (*A* and *B*) Activation of platelets stimulated with thrombin. Platelets (1.0×10^7) were stimulated with or without thrombin (1 U/mL) for 15 minutes. Shape change and P-selectin surface expression of platelets were analyzed by flow cytometry (*A*); representative data are shown; note that FSC increased with addition of thrombin; *closed histograms* and *open histograms* indicate P-selectin surface expression of platelets stimulated with or without thrombin, respectively. Soluble P-selectin levels of the culture supernatants were determined by ELISA (*B*), n = 3/group, $^*P < .05$ vs the other 2 groups. (*C*) *col1a1* And *col1a2* mRNA levels in HSCs treated with the supernatant of activated or quiescent platelets by real-time reverse-transcription polymerase chain reaction. HSCs were cocultured with or without 1.0×10^7 platelets for 6 hours in the presence or absence of thrombin (1 U/mL). In parallel, HSCs were cultured for 6 hours with the supernatants of platelets, which had been stimulated with or without thrombin (1 U/mL) for 15 minutes, n = 3/group. $^*P < .05$ vs HSC with control group and HSC with platelet supernatant group. $^{**}P < .05$ vs HSC with thrombin group.

topenic mice (Figure 6*A*). Furthermore, phosphorylation of Met protein in the liver occurred upon BDL treatment, but it was weaker in the thrombocytopenic mice than in the control littermates (Figure 6*B*). Similar attenuation of Met phosphorylation in the thrombocytopenic mice was also observed at 3 days after BDL (Supplementary Figure 2). These results indicated that BDL-induced cholestasis led to intrahepatic platelet accumulation and activated the Met signal in the liver. In contrast, both were attenuated in the liver of the thrombocytopenic mice. Furthermore, plasma HGF levels in the thrombocytopenic mice did not increase upon BDL and were evidently lower than in the control littermates (Figure 6*C*). Finally, to investigate whether attenuation of Met activation in the liver of the thrombocytopenic mice was involved in the exacerbation of liver fibrosis, we tested the hypothesis that administration of HGF, known to exert an antifibrotic effect,[20-22] would alleviate liver fibrosis in the thrombocytopenic mice more than in the control littermates. These mice were treated with either vehicle or recombinant HGF following BDL. As expected, HGF administration alleviated liver fibrosis in the thrombocytopenic mice to the level found in the control littermates (Figure 6*D*). Notably, elevated hepatic expression of type I collagen genes in the thrombocytopenic mice was also attenuated to a level comparable with that in the control littermates by the HGF therapy (Figure 6*E*).

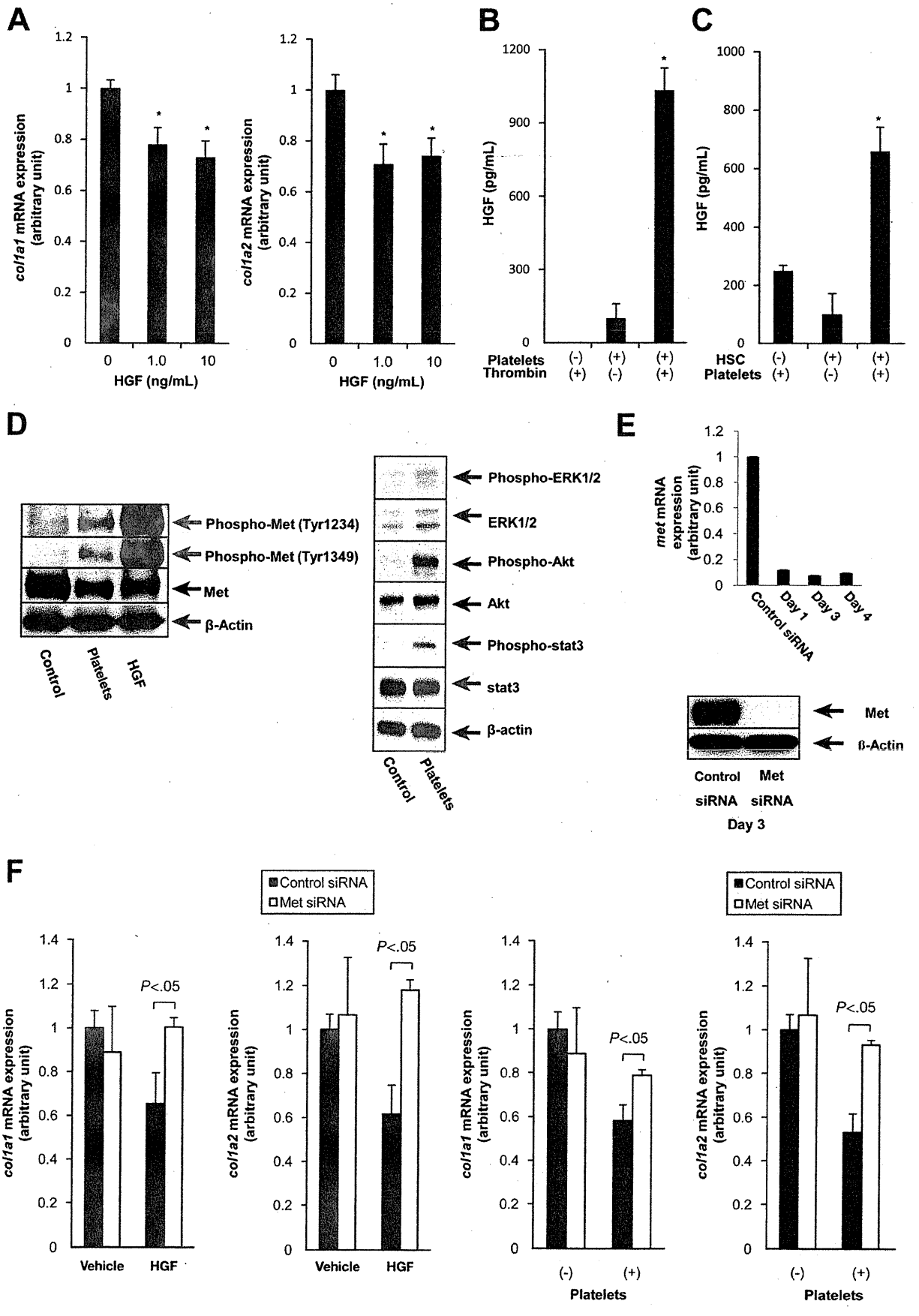
A
col1a1 mRNA expression (arbitrary unit)
HGF (ng/mL)
col1a2 mRNA expression (arbitrary unit)
HGF (ng/mL)
B
HGF (pg/mL)
Platelets
Thrombin
C
HGF (pg/mL)
HSC
Platelets
D
Phospho-Met (Tyr1234)
Phospho-Met (Tyr1349)
Met
β-Actin
Control
Platelets
HGF
Phospho-ERK1/2
ERK1/2
Phospho-Akt
Akt
Phospho-stat3
stat3
β-actin
E
met mRNA expression (arbitrary unit)
Control siRNA
Day 1
Day 3
Day 4
Met
ß-Actin
Control siRNA
Met siRNA
Day 3
F
Control siRNA
Met siRNA
col1a1 mRNA expression (arbitrary unit)
col1a2 mRNA expression (arbitrary unit)
P<.05
Vehicle
HGF
Platelets

Discussion

Platelets are circulating blood cells with the daily job of handling hemostasis and thrombosis.[14] On the other hand, they are also involved in inflammation,[23] angiogenesis, and tissue repair. Platelets have been shown to accumulate in the liver under some pathologic conditions such as acute viral hepatitis[24] and cholestasis.[25] Previous work on such situations has focused on platelets as a producer of inflammatory cytokines and on their proinflammatory role. However, a recent study has demonstrated a new role for platelets in the liver: that of platelet-derived serotonin mediating liver regeneration.[26] Moreover, it has been reported that TPO-induced thrombocytosis attenuates progression of liver fibrosis and accelerates liver fibrolysis.[27,28] However, the mechanisms remain obscure, and the extrathrombocytotic effect of TPO could not be excluded from their study results. In the present study, we were able to clearly demonstrate that platelets serve as antifibrotic cells in the liver via the HGF/Met pathway and offer the novel finding that thrombocytopenia exacerbates liver fibrosis in vivo.

To examine the impact of thrombocytopenia in liver fibrosis, we generated a novel mouse model of severe thrombocytopenia. Previous research has shown that platelets are genetically programmed to die in an apoptotic manner and that their life span is regulated by a fine balance between antiapoptotic Bcl-xL and proapoptotic Bak; mice lacking a single allele of the *bcl-x* gene develop mild thrombocytopenia, which is attenuated with a *bak* knockout background.[5] However, traditional knockout of both alleles of the *bcl-x* gene leads to embryonic lethality.[6] To develop severe thrombocytopenic mice without phenotype expression in other organs caused by Bcl-xL deficiency, we generated thrombocyte-specific Bcl-xL knockout mice by crossing *floxed bcl-x* mice[6,7] and transgenic mice expressing the Cre-recombinase under regulation of the promoter of the Pf4 gene.[8] The expression of Pf4 promoter is reported to be specific to thrombocytes,[8] and its specificity was also confirmed in our generated mice. The mice displayed severer thrombocytopenia than the single allele knockout mice, at as early as 4 weeks of age, and it persisted for a longer time (Supplementary Figure 3).

Thrombocytopenic mice did not develop any liver pathology under physiologic conditions but developed exacerbated liver fibrosis upon BDL. Similar exacerbation of liver fibrosis was found in another liver fibrosis model induced by chronic injection of carbon tetrachloride (Supplementary Figure 4). Following BDL, thrombocytopenic mice showed lower ALT levels than the control mice. Because there was no significant difference in histologic necrosis and hepatocyte apoptosis between the 2 groups, the significance of this difference is obscure. Research has revealed proinflammatory roles of platelets in the liver under some experimental conditions.[23-25] Thus, thrombocytopenia might have led to modest reduction of liver injury in our experiment without any histologic differences. Even if that were the case, modest decline of liver injury could not explain the exacerbation of liver fibrosis in thrombocytopenic mice. It is well known that the liver has the unique capacity to regenerate in response to partial hepatectomy or some types of liver injury.[29] Recent research has shown that platelets mediate liver regeneration after partial hepatectomy.[26] In our experiment, modest compensatory regeneration did occur following BDL, but we could not find any difference in liver regeneration between the 2 groups. Following two thirds' partial hepatectomy, most hepatocytes in the remaining liver enter an active state of cell cycle progression,[29] whereas only a relatively small number of them may do so following liver injury. That may explain why liver regeneration did not differ in our models. Taken together, we considered that liver fibrosis is the primary and most prominent difference between the thrombocytopenic mice and the control littermates after BDL.

With regard to the underlying mechanisms of exacerbated liver fibrosis in thrombocytopenic mice upon BDL, we first took particular notice of the increase in collagen gene expression. In fact, liver fibrosis is known to be regulated by a fine balance between fibrogenesis and fibrolysis.[1,2] A variety of matrix metalloproteases (MMPs), such as MMP-2, MMP-9, and MMP-14, which may be involved in fibrolysis, were also up-regulated in the liver in thromobocytopenic mice compared with control mice (Supplementary Figure 5*A*). In addition, gene expression of platelet-derived growth factor, D polypeptide, transforming

Figure 5. The HGF/Met pathway is involved in platelet-mediated inhibition of collagen synthesis in HSCs in vitro. (*A*) *co1a1* And *col1a2* mRNA levels in HSCs stimulated with murine HGF for 6 hours by real-time reverse-transcription polymerase chain reaction, n = 3/group. *$P < .05$ vs control. (*B*) Secretion of HGF from activated platelets. Platelets (1.0×10^7) were stimulated with or without thrombin (1 U/mL) for 15 minutes, and the levels of HGF in the culture supernatant were determined by ELISA, n = 3/group. *$P < .05$ vs other 2 groups. (*C*) Production of HGF in platelet/HSC coculture. HSCs (1.0×10^5) were cocultured with 5.0×10^7 of platelets for 3 hours, and the levels of HGF in the culture medium were determined by ELISA, n = 3/group. *$P < .05$ vs the other 2 groups. (*D*) Activation of Met and its downstream pathways in platelet/HSC coculture. HSCs (5.0×10^5) were cocultured with or without 5.0×10^7 platelets or with 20 ng/mL HGF as a positive control for 1 hour. Western blot analysis of phosphorylated Met protein at indicated position of tyrosine (*left panel*) and phosphorylated Erk1/2, Akt, and stat3 proteins (*right panel*). (*E*) Real-time reverse-transcription polymerase chain reaction (*upper panel*) and Western blot analysis (*lower panel*) of Met expression in HSCs transfected with *met* siRNA or control siRNA. (*F*) *co1a1* And *col1a2* mRNA levels in HSCs treated with *met* siRNA by real-time reverse-transcription polymerase chain reaction. HSCs were transfected with *met* siRNA or control siRNA for 3 days and then cultured for 6 hours with or without 20 ng/mL HGF (*left*) or with or without 1.0×10^7 platelets (*right*), n = 3/group.

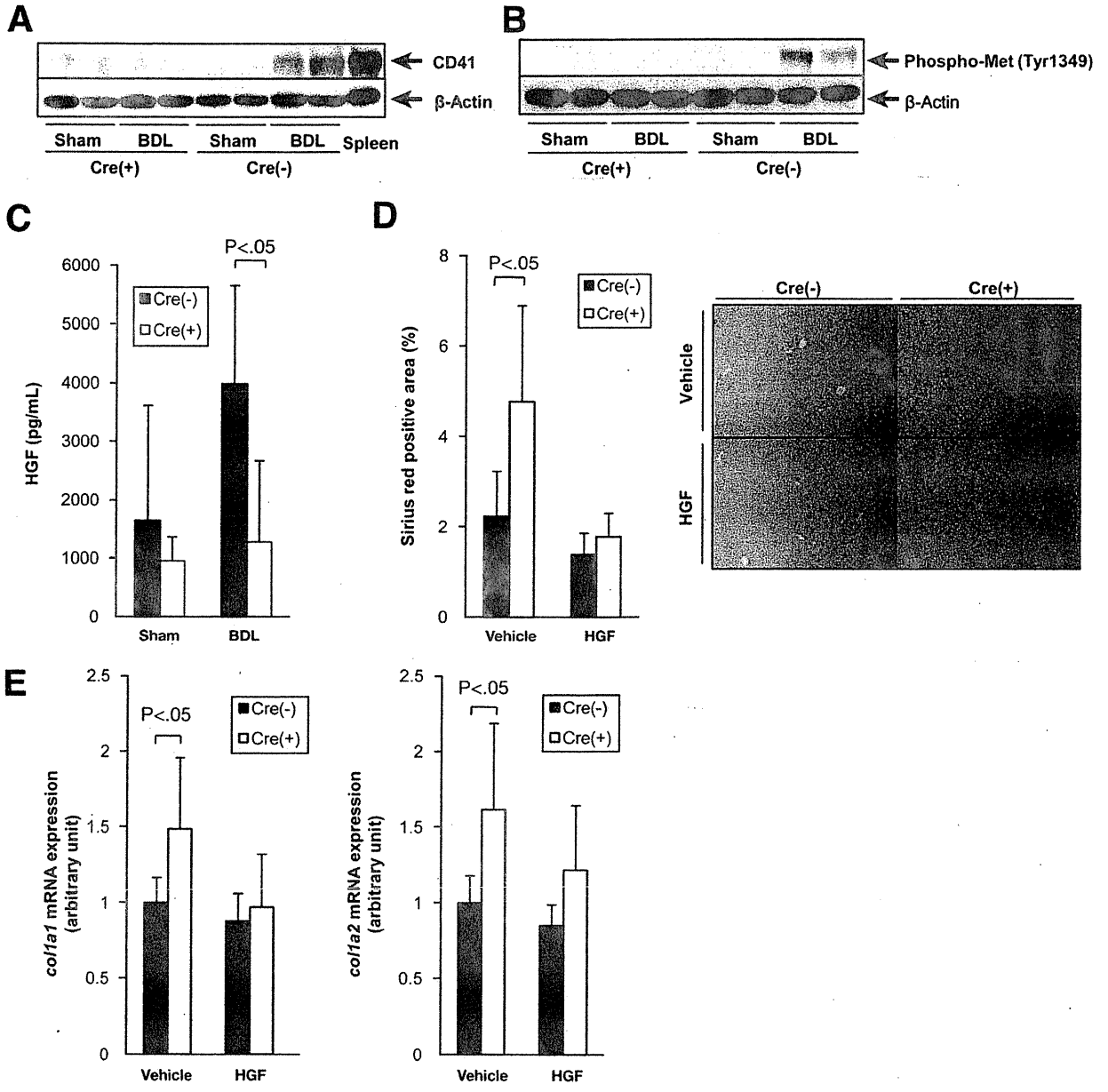

Figure 6. HGF administration prevents the exacerbation of liver fibrosis in the thrombocytopenic mice after BDL. (*A–C*) Platelet accumulation and Met activation in the liver following BDL. *bcl-x*$^{flo/xflox}$ *Pf4-Cre* mice and *bcl-x*$^{flox/flox}$ mice were sham operated or subjected to BDL and analyzed 10 days later (4–7 mice per group). Cre(+) stands for *bcl-x*$^{flox/flox}$ *Pf4-Cre* mice and Cre(−) for *bcl-x*$^{flox/flox}$ mice. Platelet accumulation in the liver was assessed by Western blotting of CD41 (*A*); lysate of spleen was used as a positive control. Phosphorylation of Met protein in the liver was determined by Western blot analysis (*B*). Plasma HGF levels were determined by ELISA (*C*). (*D* and *E*) Attenuation of liver fibrosis by HGF therapy in thrombocytopenic mice following BDL. *bcl-x*$^{flo/xflox}$ *Pf4-Cre* mice and *bcl-x*$^{flox/flox}$ mice were subjected to BDL, followed by intraperitoneal injection of recombinant human HGF or vehicle 2 times per day and analyzed 10 days later (5–7 mice per group). Liver fibrosis was evaluated by picrosirius red staining of liver sections (*D*). *col1a1* And *col1a2* mRNA in the liver were determined by real-time reverse-transcription polymerase chain reaction (*E*).

growth factor-β, and tumor necrosis factor-α, which are also known as cytokines involved in fibrosis, was not different between the 2 groups (Supplementary Figure 5*B*). These gene expression profiles suggest that increase of collagen gene expression may have a causative role in exacerbated liver fibrosis and that MMP up-regulation may be a compensatory phenomenon.

In general, according to the transdifferentiation of quiescent HSCs into activated HSCs, these myofibroblast-like cells express myogenic markers such as α-smooth muscle actin (SMA) and cause a parallel increase in collagen synthesis.[1,2] However, instead of increased collagen synthesis in thrombocytopenic mice, α-SMA positive cells were similarly induced in thrombocytopenic mice and control

mice upon BDL (Supplementary Figure 6). Thereafter, we expected that the levels of collagen gene expression per cell would increase in thrombocytopenic mice. Previous research has demonstrated that, even in activated HSCs, the level of type I collagen mRNA can be modulated by the change of collagen mRNA stabilization, which is regulated by interaction with a specific protein such as α complex protein.[30] Furthermore, it has recently been demonstrated that HGF suppresses *col1a2* promoter activation by inhibiting nuclear accumulation of Smad3 in activated HSCs.[31] We used activated HSCs for in vitro experiments and found that coculture with platelets did not affect mRNA expression of α-SMA (Supplementary Figure 7) but did suppress the *col1a1* and *col1a2* genes in activated HSCs. This suggests that platelets regulate type I collagen gene expression in each cell without affecting the activation status of HSCs, which agrees with our in vivo findings.

Platelet suppression of collagen gene expression was clearly associated with platelet activation as evidenced by the shape change and P-selectin translocation and shedding. Moreover, the supernatant of thrombin-activated platelets was capable of inhibiting collagen gene expression, although the supernatant of quiescent platelets could not. These results strongly suggest that platelet activation is indispensable for the inhibition of collagen synthesis in vitro. It should be noted that our results also suggest that, once activated, platelets are capable of releasing soluble factor(s) residing in platelet granules such as HGF and thereby suppress collagen synthesis, which is independent of how platelets are activated. Therefore, although platelets could be activated upon contact with HSCs in vitro, this contact may not be a requisite for platelet inhibition of HSCs in vivo. Indeed, platelets are well known to be activated by cell-to-cell contact with a variety of cells and soluble factors in injured organs.[10,14] We also observed that platelets could be activated upon contact with murine hepatocytes or macrophages in vitro, even though activated platelets did not affect type I collagen synthesis in these cells (data not shown).

We have demonstrated that platelet-derived HGF plays a critical role in platelet suppression of type I collagen gene expression in cultured HSCs. BDL-induced cholestasis led to intrahepatic platelet accumulation and Met phosphorylation in the liver of control mice, but both were attenuated in thrombocytopenic mice. Furthermore, plasma HGF levels in thrombocytopenic mice were lower than in control mice after BDL. Despite the lack of intrahepatic platelet accumulation, HGF administration could alleviate cholestasis-induced liver fibrosis in thrombocytopenic mice to the same level found in control mice. These findings implied that the lack of platelet-derived HGF signaling in the liver was involved in exacerbated liver fibrosis in thrombocytopenic mice. It is not clear, in the present study, whether cholestasis-induced Met phosphorylation in the liver originates from activated HSCs or just hepatocytes. Therefore, it is quite possible that HGF administration alleviated liver fibrosis by stimulating both hepatocytes and HSCs in thrombocytopenic mice. However, marked suppression of hepatic type I collagen gene expression by HGF therapy in thrombocytopenic mice suggests that attenuated Met phosphorylation and the subsequent increase of collagen synthesis in activated HSCs may be involved in exacerbated liver fibrosis in thrombocytopenic mice because collagen production is mainly mediated by activated HSCs in the injured liver.

HGF was first identified as a potent mitogen for primary hepatocytes after being purified from the plasma of a patient with fulminant hepatic failure[16,17] and also from rat platelets.[18] HGF is known to be a multifunctional growth factor that shows mitogenic, motogenic, morphogenic, and antiapoptotic activities in a variety of cells.[16,17] Increasing evidence indicates that HGF has an antifibrotic effect in several experimental models, especially when administered exogenously.[20,21] Although platelets are known to contain HGF in their granules,[18] the functional role of platelet-derived HGF has remained unknown. Because human platelets contain a smaller amount of HGF than rodent platelets,[18] it is obscure whether the same mechanisms observed in rodents are operative in humans. However, the present study, for the first time, sheds light on HGF derived from platelets serving as an endogenous negative regulator for HSC expression of collagen genes and liver fibrosis under pathologic conditions.

Thrombocytopenia is a common complication of advanced chronic liver disease and is generally considered to be a secondary phenomenon via associated portal hypertension or reduced production of TPO in the liver.[3,4] Our study indicates a causal link of thrombocytopenia with progression of liver fibrosis, suggesting a complicated interaction between liver fibrosis and thrombocytopenia. However, the mice we generated show extremely severe thrombocytopenia, which does not exactly mimic the thrombocytopenia usually seen in patients with cirrhosis. Moreover, the components of platelet granules may differ between the human and the mouse. Therefore, we cannot directly conclude from our findings that thrombocytopenia in patients with cirrhosis exacerbates liver fibrosis. However, in addition to the fact that liver fibrosis progresses in parallel with the decrease of platelet count, several studies on human patients have shown that splenectomy or partial splenic embolization can improve the liver function of cirrhotic patients in parallel with elevation of platelet count.[32,33] Therefore, further clinical study is important in order to elucidate whether an increase in platelet count is beneficial for preventing the progression of liver fibrosis in thrombocytopenic patients with advanced liver disease.

Supplementary Material

Note: To access the supplementary material accompanying this article, visit the online version of *Gastroenterology* at www.gastrojournal.org, and at doi: 10.1053/j.gastro.2010.02.054.

References

1. Bataller R, Brenner DA. Liver fibrosis. J Clin Invest 2005;115: 209–218.
2. Friedman SL. Mechanisms of hepatic fibrogenesis. Gastroenterology 2008;134:1655–1669.
3. Afdhal N, McHutchison J, Brown R, et al. Thrombocytopenia associated with chronic liver disease. J Hepatol 2008;48:1000–1007.
4. Aster RH. Pooling of platelets in the spleen: role in the pathogenesis of "hypersplenic" thrombocytopenia. J Clin Invest 1966;45: 645–657.
5. Mason KD, Carpinelli MR, Fletcher JI, et al. Programmed anuclear cell death delimits platelet life span. Cell 2007;128:1173–1186.
6. Takehara T, Tatsumi T, Suzuki T, et al. Hepatocyte-specific disruption of Bcl-xL leads to continuous hepatocyte apoptosis and liver fibrotic responses. Gastroenterology 2004;127:1189–1197.
7. Hikita H, Takehara T, Shimizu S, et al. Mcl-1 and Bcl-xL cooperatively maintain integrity of hepatocytes in developing and adult murine liver. Hepatology 2009;50:1217–1226.
8. Tiedt R, Schomber T, Hao-Shen H, et al. Pf4-Cre transgenic mice allow generating lineage-restricted gene knockouts for studying megakaryocyte and platelet function in vivo. Blood 2007;109: 1503–1506.
9. Tsukamoto H, Matsuoka M, French SW. Experimental models of hepatic fibrosis: a review. Semin Liver Dis 1990;10:56–65.
10. Zarbock A, Polanowska-Grabowska RK, Ley K. Platelet-neutrophil-interactions: linking hemostasis and inflammation. Blood Rev 2007;21:99–111.
11. Bennet JS. Structure and function of the platelet integrin αIIbβ3. J Clin Invest 2005;115:3363–3369.
12. Gujral JS, Liu J, Farhood A, et al. Reduced oncotic necrosis in Fas receptor-deficient C57BL/6J-lpr mice after bile duct ligation. Hepatology 2004;40:998–1007.
13. Friedman SL, Roll FJ, Boyles J, et al. Maintenance of differentiated phenotype of cultured rat hepatic lipocytes by basement membrane matrix. J Biol Chem 1989;264:10756–10762.
14. Holmsen H. Physiological functions of platelets. Ann Med 1989; 21:23–30.
15. Dunlop LC, Skinner MP, Bendall LJ, et al. Characterization of GMP-140 (P-selectin) as a circulating plasma protein. J Exp Med 1992;175:1147–1150.
16. Gohda E, Tsubouchi H, Nakayama H, et al. Purification and partial characterization of hepatocyte growth factor from plasma of a patient with fulminant hepatic failure. J Clin Invest 1988;81: 414–419.
17. Miyazawa K, Tsubouchi H, Naka D, et al. Molecular cloning and sequence analysis of cDNA for human hepatocyte growth factor. Biochem Biophys Res Commun 1989;163:967–973.
18. Nakamura T, Nishizawa T, Hagiya M, et al. Molecular cloning and expression of human hepatocyte growth factor. Nature 1989; 342:440–443.
19. Tulasne D, Foveau B. The shadow of death on the MET tyrosine kinase receptor. Cell Death Differ 2008;15:427–434.
20. Ueki T, Kaneda Y, Tsutsui H, et al. Hepatocyte growth factor gene therapy of liver cirrhosis in rats. Nat Med 1999;5:226–230.
21. Li Z, Mizuno S, Nakamura T. Antinecrotic and antiapoptotic effects of hepatocyte growth factor on cholestatic hepatitis in a mouse model of bile-obstructive diseases. Am J Physiol Gastrointest Liver Physiol 2007;292:G639–G646.
22. Giebeler A, Boekschoten MV, Klein C, et al. c-Met confers protection against chronic liver tissue damage and fibrosis progression after bile duct ligation in mice. Gastroenterology 2009;137: 297–308.
23. Iannacone M, Sitia G, Isogawa M, et al. Platelets mediate cytotoxic T lymphocyte-induced liver damage. Nat Med 2005;11: 1167–1169.
24. Lang PA, Contaldo C, Georgiev P, et al. Aggravation of viral hepatitis by platelet-derived serotonin. Nat Med 2008;14:756–761.
25. Laschke MW, Dold S, Menger MD, et al. Platelet dependent accumulation of leukocytes in sinusoids mediates hepatocellular damage in bile duct ligation-induced cholestasis. Br J Pharmacol 2008;153:148–156.
26. Lesurtel M, Graf R, Aleil B, et al. Platelet-derived serotonin mediates liver regeneration. Science 2006;312:104–107.
27. Murata S, Hashimoto I, Nakano Y, et al. Single administration of thrombopoietin prevents progression of liver fibrosis and promotes liver regeneration after partial hepatectomy in cirrhotic rats. Ann Surg 2008;248:821–828.
28. Watanabe M, Murata S, Hashimoto I, et al. Platelets contribute to the reduction of liver fibrosis in mice. J Gastroenterol Hepatol 2009;24:78–89.
29. Fausto N, Campbell JS, Riehle KJ. Liver regeneration. Hepatology 2006;43:S45–S53.
30. Stefanovic B, Hellebrand C, Holcik M, et al. Posttranscriptional regulation of collagen α1(I) mRNA in hepatic stellate cells. Mol Cell Biol 1999;17:5201–5209.
31. Inagaki Y, Higashi K, Kushida M, et al. Hepatocyte growth factor suppresses profibrogenic signal transduction via nuclear export of smad3 with galectin-7. Gastroenterology 2008;134:1180–1190.
32. Murata K, Ito K, Yoneda K, et al. Splenectomy improves liver function in patients with liver cirrhosis. Hepatogastroenterology 2008;55:1407–1411.
33. Lee CM, Leung EK, Wang HJ, et al. Evaluation of the effect of partial splenic embolization of platelet values for liver cirrhosis patients with thrombocytopenia. World J Gastroenterol 2007;13: 619–622.

Received September 4, 2009. Accepted February 24, 2010.

Reprint requests

Address requests for reprints to: Norio Hayashi, MD, PhD, Department of Gastroenterology and Hepatology, Osaka University Graduate School of Medicine, 2-2 Yamada-oka, Suita, Osaka 565-0871, Japan. e-mail: hayashin@gh.med.osaka-u.ac.jp; fax: (81) 6-6879-3629.

Acknowledgments

The authors thank Radek Skoda (University Hospital Basel) and Lothar Hennighausen (National Institute of Health) for providing the *Pf4-Cre* mice and the *floxed bcl-x* mice, respectively.

T. Kodama and T. Takehara contributed equally to this work and share first authorship.

Conflicts of interest

The authors disclose no conflicts.

Funding

Supported in part by a Grant-in-Aid for Scientific Research from the Ministry of Education, Culture, Sports, Science, and Technology, Japan (to T. Takehara), and a Grant-in-Aid from the Ministry of Health, Labour, and Welfare of Japan.

Supplementary Materials and Methods

Hematologic Analyses

Blood was collected from the inferior vena cava of mice. Complete blood cell counts were determined using an Automated Cell Counter (Sysmex, Kobe, Japan).

Histologic Analyses

The liver sections were stained with H&E or picrosirius red. The percentage of oncotic necrosis or fibrotic area was calculated using image analysis software (winROOF visual system; Mitani Co, Tokyo, Japan). To assess intrahepatic neutrophil accumulation, liver sections were stained with chloroacetate esterase, which is a specific marker of neutrophils,[1] using a Naphthol-ASD Chloroacetate Esterase Kit (Sigma–Aldrich, St. Louis, MO). To detect apoptotic cells, the liver sections were also subjected to terminal deoxynucleotidyl transferase-mediated deoxyuridine triphosphate nick-end labeling staining as previously reported.[2] To assess regenerative status, nuclear 5-bromo-2-deoxyuridine incorporation was evaluated as previously described.[3]

Determination of Liver Hydroxyproline Content

Hydroxyproline content was determined essentially as described previously.[4] Results are expressed as micrograms of hydroxyproline per gram of wet liver.

Isolation and Culture of Mouse Hepatic Stellate Cell

Hepatic stellate cell (HSCs) were isolated from C57BL/6J mice by 2-step collagenase-pronase perfusion of mouse liver followed by density gradient centrifugation with 8.2% Nycodenz (Sigma–Aldrich) as previously described.[5] Isolated HSCs were maintained at 37°C under 5% CO_2 in Dulbecco's modified Eagle medium containing 10% fetal calf serum. Activated HSCs after a few passages were used for the experiments unless otherwise indicated.

Cell Isolation

Monocytes and T lymphocytes were isolated from spleens of *bcl-x$^{flox/flox}$ Pf4-Cre* mice and *bcl-x$^{flox/flox}$* mice by magnetic cell sorting using magnetic beads (MACS; Miltenyi Biotec, Gladbach, Germany) with CD11b and CD90.2 antibodies according to the manufacturer's protocol. Abdominal macrophages were collected from these mice 5 days after intraperitoneal injection of 50 μL/g body weight thioglycollate broth (Sigma–Aldrich) by peritoneal lavage. Hepatocytes and nonparenchymal cells were isolated from those mice by collagenase perfusion of mouse liver followed by centrifugation.

Platelet Isolation

Platelets were isolated as described previously.[6] Briefly, whole blood collected from the inferior vena cava of C57BL/6J mice was mixed with one fourth volume of citrate phosphate dextrose (Sigma–Aldrich). Platelet-rich plasma was obtained by centrifugation at 100*g* for 15 minutes at room temperature without braking. After incubation with 1 μmol/L prostaglandin E_1 (Sigma–Aldrich) and 1 U/mL apyrase (Sigma–Aldrich), the platelets were isolated by centrifugation at 200*g* at room temperature for 15 minutes.

Western Blot Analysis

Western blotting was performed as previously described.[2] A detailed description of the antibodies used is provided in Supplementary Table 1.

Real-Time Reverse-Transcription Polymerase Chain Reaction

Total RNA extracted from the liver tissue and HSCs were reverse transcribed and subjected to real-time reverse-transcription polymerase chain reaction as previously described.[2] mRNA expression of the specific genes was quantified using TaqMan Gene Expression Assays (Applied Biosystems Inc, Foster City, CA). Assay IDs of the specific genes are provided in Supplementary Table 2. Transcript levels are presented as fold induction.

Small Interfering RNA-Mediated Knockdown

Cultured HSCs were transfected with small interfering RNA against *met* (Stealth RNAi, Oligo ID:MSS206635) (Invitrogen, Carlsbad, CA) using lipofectamine RNAi-MAX (Invitrogen) according to the manufacturer's protocol. Stealth RNA: Negative Control Low GC Duplex (Invitrogen) was used as the control.

Flow Cytometry

Isolated platelets were surface-stained with a fluorescein isothiocyanate-conjugated rat anti-mouse CD62p (P-selectin) antibody (BD Biosciences, Franklin Lakes, NJ). Samples were analyzed with a Becton Dickinson FACSCalibur flow cytometer (BD Biosciences), and the data were processed with the CELLQuest software (BD Biosciences).

Enzyme-Linked Immunosorbent Assay

Mouse HGF and soluble CD62p (P-selectin) levels in plasma and culture supernatant were measured by using DuoSet enzyme-linked immunosorbent assay mouse hepatocyte growth factor (HGF) and CD62p (R&D Systems, Minneapolis, MN), respectively, according to the manufacturer's protocol.

HGF Treatment

Wild-type (*bcl-x$^{fl/fl}$*) and knockout (*bcl-x$^{fl/fl}$ Pf4-Cre*) mice were subjected to bile duct ligation, followed by intraperitoneal injection of recombinant human HGF (500 μg/kg) or vehicle every 12 hours for 10 days and then killed to sample the liver tissues.

References

1. Gujral JS, Liu J, Farhood A, et al. Reduced oncotic necrosis in Fas receptor-deficient C57BL/6J-lpr mice after bile duct ligation. Hepatology 2004;40:998–1007.
2. Hikita H, Takehara T, Shimizu S, et al. Mcl-1 and Bcl-xL cooperatively maintain integrity of hepatocytes in developing an adult murine liver. Hepatology 2009;50:1217–1226.
3. Lesurtel M, Graf R, Aleil B, et al. Platelet-derived serotonin mediates liver regeneration. Science 2006;312:104–107.
4. Takehara T, Tatsumi T, Suzuki T, et al. Hepatocyte-specific disruption of Bcl-xL leads to continuous hepatocyte apoptosis and liver fibrotic responses. Gastroenterology 2004;127:1189–1197.
5. Seki E, De Minicis S, Osterreicher CH, et al. TLR4 enhances TGF-β signaling and hepatic fibrosis. Nat Med 2007;13:1324–1332.
6. Iannacone M, Sitia G, Isogawa M, et al. Platelets mediate cytotoxic T lymphocyte-induced liver damage. Nat Med 2005;11:1167–1169.